POLITECNICO DI TORINO

Collegio di Ingegneria Chimica e dei Materiali

Master of Science Course
in Materials Engineering

Master of Science Thesis

Towards customisable fully composite bone fracture fixators

Tutors
prof. Marco Sangermano[1]
prof. Michael Malkoch[2]

Supervisors
Daniel J. Hutchinson[1]
Jorge San Jacinto Garcia[1]

Candidate
Lorenzo Papini

[1]Department of Applied Science and Technology, Politecnico di Torino
[2]Division of Coating Technology, KTH Royal Institute of Technology

July 2023

List of abbreviations

BFP	Bone fixation patch
Bgl	Bioactive glass
β-TCP	β-Tricalcium phosphate
CDI	N, N-carbonyl diimidazole (1,1′-Carbonyldiimidazole)
DMSO	Dimethylsulfoxide
DTNB	5,5′-Dithiobis(2-nitrobenzoic acid)
ERS	Ellman’s reagent solution
EtOAc	Ethyl acetate
EtOH	Ethanol
13C-NMR	Carbon-13 nuclear magnetic resonance spectroscopy
FBR	Foreign body reaction
FRAP	Fibre reinforced adhesive patch
FT-RAMAN	Fourier transform Raman spectroscopy
FT-IR	Fourier transform infrared spectroscopy
HA	Hydroxyapatite
HA-w	Hydroxyapatite whiskers
HEV	High energy visible (light)
1H-NMR	Proton nuclear magnetic resonance spectroscopy
LED	Light-emitting diode
MgSO4	Magnesium sulphate
γ-MPS	γ-methacryloxypropyltrimethoxysilane or 3-(trimethoxysilyl)propyl methacrylate
ORIF	Open reduction internal fixation
PMC	Polymer matrix composite
PRPMC	Particulate reinforced polymer matrix composite
SEM	Scanning electron microscopy
SSA	Specific surface area
TATO	1,3,5,-Triazine-2,4,6-trione
TATATO	1,3,5-Triallyl-1,3,5-triazine-2,4,6-trione

TE	Thiol-ene
TEMPIC	Tris(2-mercaptopropinyloxy) ethyl isocyanurate
TMTATO	1,3,5-triazine-2,4,6-trione, 1,3,5-tris(mercaptopropyl)
TPO	Diphenyl(2,4,6-trimethylbenzoyl) phosphine oxide
PEMPA	((pent-4-enoyloxy)methyl)phosphonic acid
PEMPA-Et	(diethoxyphosphoryl)methyl pent-4-enoate
UEMPA	((undec-10-enoyloxy)methyl)phosphonic acid
UEMPA-Et	(diethoxyphosphoryl)methyl undec-10-enoate
UV	Ultraviolet

Riassunto esteso

I. Introduzione e background

I.i Fissazione di fratture ossee e fratture della mano

La prime notizie sull' utilizzo di dispositivi metallici per la fissazione di fratture ossee si hanno già alla fine del XVIII secolo [4]. Da allora, la ricerca nel campo della chirurgia e della scienza dei materiali ha portato a enormi miglioramenti nelle tecniche chirurgiche e nelle proprietà delle leghe metalliche, anche per usi biomedicali. Perni, fili, placche e viti sono oggi disponibili in un'ampia gamma di forme, dimensioni e leghe, generalmente a base di titanio o acciaio inossidabile, che vengono selezionate in base alle specifiche necessità del caso chirurgico. Di fatto, gli impianti metallici rappresentano lo stato dell'arte per la fissazione di fratture ossee instabili che richiedono un interventodi osteosintesi con fissazione interna. Tuttavia, nonostante gli eccezionali progressi e l'ampia diffusione, questi dispositivi non sono esenti da complicazioni, che possono variare, anche significativamente, a seconda del caso di applicazione specifico.

Gli inconvenienti più comuni degli impianti metallici rientrano nella categoria delle reazioni da corpo estraneo (FBR). La FBR è innescata dall'adsorbimento competitivo e dalla successiva denaturazione delle proteine sulla superficie del materiale. Questo processo avvia una cascata di segnali che porta alla risposta immunitaria, all'infiammazione, alla formazione di granulomi e infine all'incapsulamento fibroso [5]. La FBR è modulata da una serie di diversi fattori diversi, quali la chimica superficiale, la sua rugosità, la tribologia complessiva, la geometria dell'impianto e le sue proprietà meccaniche [6]. Nelle situazioni più gravi, ciò può portare a dolore intenso, ad un'infiammazione cronica, o addirittura alla necessità di un secondo intervento con il rischio tangibile di causare danni permanenti all'area interessata. Un danneggiamento locale dei tessuti può anche essere causato dal rilascio di ioni o particelle metalliche in seguito ad usura localizzata o ad ossidazione. [7,8]

I dispositivi metallici disponibili in commercio hanno un modulo di elasticità significativamente più elevato rispetto all'osso (e.g. Ti6Al4V 116 GPa contro 5-23GPa dell'osso corticale). Questo porta, soprattutto qundo sostengono carichi meccanici, a far sì che la maggior parte di questo sia sostenuto dall'impianto piuttosto che dall'osso, una situazione denominata "stress shielding" che a sua volta causa una riduzione della densità ossea circostante (osteopenia) [7,8] . Dal punto di vista chirurgico invece, lo svantaggio principale è che le placche metalliche sono intrinsecamente non personalizzabili durante l'intervento a causa della loro rigidità, rendendo complicato e meno soddisfacente il loro utilizzo quando i segmenti ossei presentano conformazioni particolari.

Si stima che nel 2019 soltanto, si siano verificate 178 milioni di fratture ossee nel mondo, in aumento di oltre il 30% dal 1990 [1]. Tra tutti le diverse tipologie, le fratture coinvolgenti le ossa falangee o metacarpali sono tra le più comuni. Sono ad esempio le più frequenti nella fascia di età compresa tra i 18 e i 35 anni negli Stati Uniti d'America, rappresentando oltre il 50% di tutte le fratture in questa fascia di età [9]. Nel 1996, nel dipartimento pronto soccorso

del VU University Medical Centre di Amsterdam, le fratture delle falangi o dei metacarpi rappresentavano il 19% del totale dei casi di frattura [10]. Inoltre, queste fratture espongono i pazienti a un elevato rischio di complicazioni postoperatorie. Le stime su tali complicanze riportano valori differenti a seconda della complessità della frattura, del tipo di fissazione, e della coorte considerata. Per dare un'idea delle dimensioni del fenomeno, l'ordine di grandezza per tutte le fratture alle mani si aggira sul 30-50% di complicanze maggiori, che salgono oltre il 60% considerando le fratture falangee fissate con placche e viti metalliche, il sistema con maggior frequenza di complicanze [2,11]. Le più comuni includono rigidità, sindrome dolorosa regionale complessa, infezione, unione ritardata, mancata unione, malunione e mobilizzazione della placca [11,12]. Questi problemi portano spesso alla necessità di un nuovo intervento, comeaccade fino al 42% dei casi per le fratture delle falangi trattate con la fissazione della placca[13].

I.i.a Fili di Kirschner (K-wire)

I fili di Kirschner, anche detti K-wire, sono dei fili rigidi ed appuntiti alle estremità, in acciaio inossidabile, che vengono comunemente impiegati come fissatori nelle fratture della mano. Il loro utilizzo prevede generalmente un inserimento percutaneo guidato tramite raggi-x attraverso i frammenti ossei che devono essere mantenuti allineati. Possono essere utilizzate varie geometrie e configurazioni, con fili singoli o multipli, a seconda del caso e del giudizio del chirurgo. I K-wires hanno diversi lati positivi: la procedura è generalmente breve e l'inserimento percutaneo, piuttosto che una riduzione aperta, limita il danno ai tessuti molli circostanti; la rimozione è rapida e facile poiché parte del k-wire rimane esposta; infine, sono economici. D'altro canto, sono generalmente in grado di mantenere solo l'allineamento delle ossa, ma non di mantenere la compressione tra di esse e non riescono a sopportare sollecitazioni a flessione. Per questo motivo, spesso necessitano di un'ulteriore immobilizzazione esterna, come un'ingessatura o una steccatura, che non consente una significativa mobilitazione precoce, aumentando sostanzialmente il rischio di adesione tendinea e di futura riduzione della mobilità. Altri problemi sono la migrazione del filo che causa malunioni, l'infezione del setto del filo e, occasionalmente, la sindrome da dolore regionale complesso. [14,15]

I.i.b Riduzione aperta e fissazione interna(ORIF)

La riduzione aperta con fissazione interna (ORIF) nelle fratture della mano prevede generalmente l'uso di placche e viti metalliche per fissare i pezzi ossei nella posizione desiderata. Per fratture falangee e metacarpali, l'intervento viene eseguito dal lato dorsale per la facilità di accesso alle ossa, riducendo l'entità del danno ai tessuti molli che seguirebbe ad un approccio palmare. Ciò limita significativamente lo spessore della placca, poiché la frizione esercitata sui tendini estensori può compromettere il loro scorrimento, con conseguente irritazione o formazione di borsite [16]. Ciò ha portato allo sviluppo di placche con a profilo ridotto(1,1-1,3 mm) rispetto a quelle precedentemente utilizzate, dette "placche a compressione dinamica", da 2.7 mm, maggiormente indicate in casi particolari [17,18]. Altri svantaggi dei fissaggi con placche e viti metalliche sono legati alla FBR e all'adesione tendinea, che ostacola completo il recupero della mobilità, e ai danni ai tessuti molli causati dalle viti bicorticali che sporgono dall'osso, che possono portare a danni o rotture del tendine tensore[19]. Per questi motivi, i sistemi a placca sono generalmente sottoposti a un secondo intervento chirurgico per la rimozione dopo la guarigione della frattura. La resistenza e rigidità dei sistemi a placche e viti, tuttavia, consente una fissazione più stabile, in grado di

sostenere le normali sollecitazioni a flessione, permettendo quindi una precoce mobilizzazione delle articolazioni, considerata un parametro fondamentale per un recupero ottimale della mobilità.

I.ii AdhFix

Nel campo della riparazione dei tessuti ossei, il gruppo di ricerca guidato dal prof. Malkoch ha sviluppato un sistema innovativo, chiamato AdhFix, per la fissazione delle fratture basato su monomeri derivati dalla molecola 1,3,5-triazinane-2,4,6-trione (TATO). Questo metodo è adatto alle fratture che richiedono una ORIF e prevede la miscelazione di TATO-tioli e TATO-alcheni trifunzionali con un fotoiniziatore ed particelle inorganiche come rinforzanti. Si ottiene così una consistenza simile ad un dentifricio fluido che può essere modellato in base alle esigenze del chirurgo e adattato in modo paziente-specifico. Questa pasta composita viene applicata nel modo illustrato in *Figura 1* [3] e fotopolimerizzata in situ strato per strato fino all'ottenimento di un patch spesso circa 2 mm. Una descrizione dettagliata della procedura AdhFix è presentata nelle sezioni 3.2.1 e 3.2.3 della tesi, essendo parte di questa ricerca.

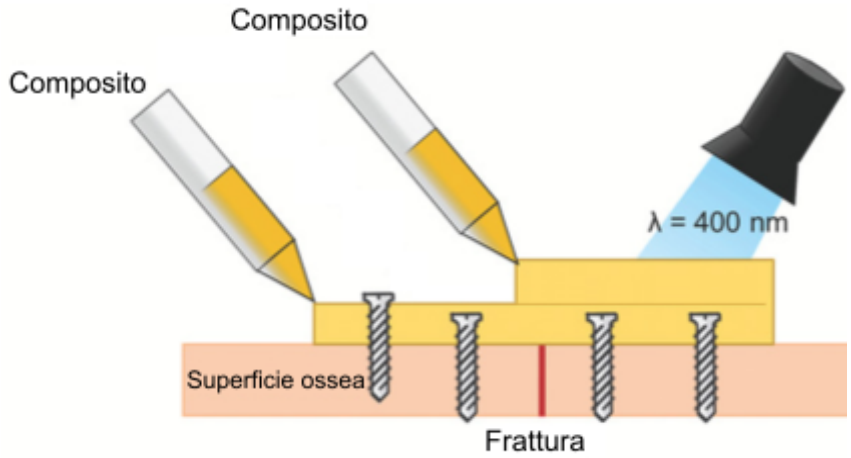

Figura I.ii: Illustrazione della tecnica strato-per strato AdhFix [3]

L'obiettivo finale del gruppo di ricerca è quello di riuscire a fissare le fratture ossee adesivamente, senza la necessità di utilizzare viti, con un sistema completamente bioriassorbibile. Le sfide per lo sviluppo di un sistema così avanzato sono numerevoli: nonostante Granskog et al.[20] abbiano sviluppato adesivi ossei significativamente superiori a quelli commercialmente disponibili, la loro performace non è ancora ritenuta abbastanza affidabile per essere utilizzata in applicazioni cliniche e non sono bioriassorbibili. Per garantire il fissaggio all'osso sottostante, è stata sviluppata il metodo AdhFix con viti corticali metalliche. Attualmente, i principali vantaggi sono la possibilità senza precedenti per i chirurghi di personalizzare la geometria del materiale in situ e le pressochè nulle adesioni tendinee, migliorando il recupero della mobilità. Tuttavia, sia per la presenza di viti metalliche sia per la natura inerte del composito, esso non è ancora bioriassorbibile [3]. Inoltre, l'interfaccia tra le viti metalliche ed il materiale composito è un punto critico, nel quale, in alcuni test preliminari, il composito si frattura.

I.ii.a Reazioni Tiolo-ene

La “chimica tiolo-ene” (TE) si riferisce a una versatile classe di reazioni che è nota fin dall'inizio del XX secolo, come riportato in un articolo ampiamente citato di Theodor Posner [21]. Grazie alla loro versatilità, aal'alta efficienza ed alle blande condizioni di reazione necessarie, ha risvegliato un crescente interesse. Come suggerisce il nome, queste reazioni comportano la reazione tra alcheni e molecole contenenti tioli e sono ampiamente suddivise in due categorie in base al meccanismo di reazione: un nucleofilo (più comunemente una base) promuove le reazioni di "addizione di thia-Michael", mentre un iniziatore radicalico induce le reazioni tiolo-ene "classiche".

Questa distinzione deriva dalla reattività pressoché opposta dei diversi alcheni nei confronti dei tioli quando subiscono reazioni anioniche piuttosto che radicaliche.

Le reazioni tiolo-ene "classiche" si avvalgono di un opportuno iniziatore radicale, generalmente foto- o termo- attivato (e.g. AIBN, derivati del benzofenone, ecc.) e seguono un particolare meccanismo a "doppio anello", come illustrato nella Figura 2 [22]. Il radicale iniziatore reagisce strappando un idrogeno dal gruppo sulfidrile, formando un radicale tiolico reattivo che si propaga tramite addizione radicalica anti-Markovnikov al legame insaturo dell'alchene per formare un radicale alchilico tioetere. Dopo questa fase, esistono due possibilità:

Omopolimerizzazione: Il radicale alchilico continua a propagarsi reagendo con altri alcheni, in modo analogo alla polimerizzazione a catena o “chain-growth”.

Trasferimento di catena: Il radicale alchilico strappa un idrogeno da un tiolo disponibile, completando di fatto un ciclo dell’anello sinistro in Figura 2, formando nuovamente un radicale tiolico libero di reagire con l'alchene successivo. Questo percorso porta a una polimerizzazione di tipo step-growth.

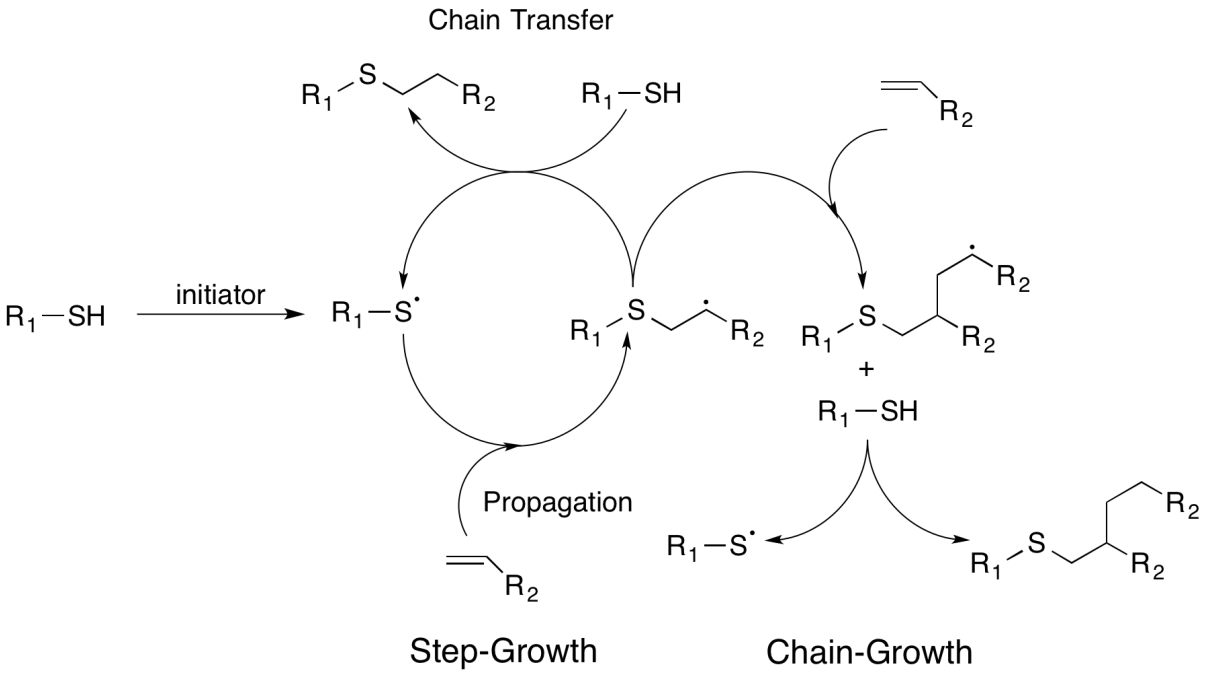

Figura I.ii.a: Meccanismo di reazione tiolo-ene [22]

II. Obiettivo e metodi

II.i Obiettivo e struttura della ricerca

Basandosi sull'attuale tecnologia AdhFix, l'obbiettivo di questo progetto è quello di sostituire le viti metalliche con viti in materiale composito a matrice tiol-enica come primo passo verso la completa riassorbibilità. Per raggiungere questo obiettivo, si è reso necessario lo sviluppo di nuove formulazioni con proprietà meccaniche migliorate. Un ulteriore passo è stato fatto includendo componenti riassorbibili. Il carico di lavoro è stato strutturato secondo tre macroaree:

1. **Formulazioni con nuovi rinforzanti:** È stato eseguito uno screening di quali filler potessero garantire il maggior rinforzo o maggior riassorbibilità al composito finale. Osservazioni al SEM sono state di supporto per la comprensione dei meccanismi di rinforzo dei diversi filler.
2. **Riduzione della porosità del materiale:** Mediante un trattamento in vuoto il materiale è stato degasato sia per aumentarne le proprietà meccaniche sia per ridurre la presenzza di difetti critici nelle viti di piccole dimensioni.
3. **Compatibilizzazione dei rinforzanti:** I due filler più promettenti sono stati sottoposti a funzionalizzazione superficiale con agenti compatibilizzanti, nell'ottica di migliorare il trasferimento di carichi con la matrice, e di conseguenza la resistenza del composito.

In seguito, la formulazione più promettente è stata utilizzata per produrre viti in composito di diverso diametro tramite iniezione con una siringa in stampi di silicone. Queste viti sono poi state utilizzate insieme alla nuova formulazione per fissare con metodo AdhFix dei modelli di frattura trasversale su metacarpi suini e testate a flessione.

II.ii Fabbricazione del composito

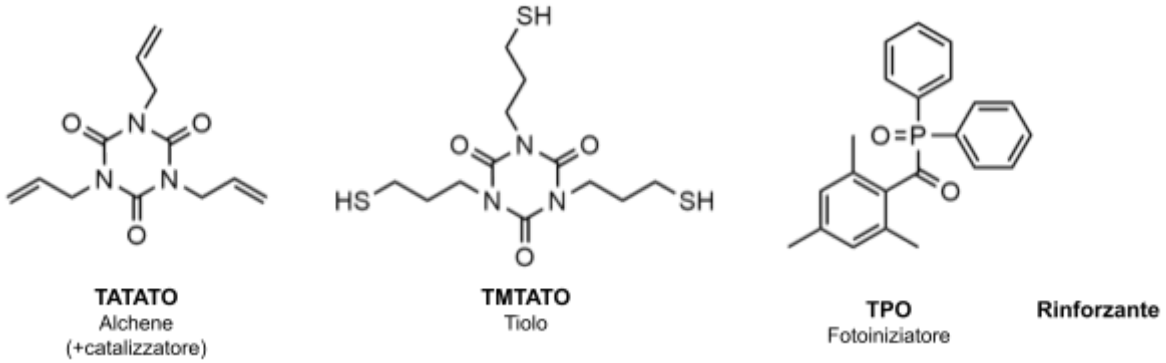

La formulazione prototipo per il composito adesso in uso per AdhFix contiene gli ingredienti di cui sopra e viene preparato come segue. Una soluzione di TATATO (12.4 g) e catalizzatore (0.7 g) (TATATO+cat) è già pronta e può essere conservata a temperatura ambiente. Il TMTATO (1810 mg) e la soluzione precostituita di TATATO+cat (1310 mg) vengono miscelati in una fiala di vetro con una pipetta di vetro chiusa. La fiala viene poi avvolta in un foglio di alluminio e il fotoiniziatore, TPO (17.8 mg), viene incorporato

mescolando con la pipetta di vetro chiusa per circa 1 minuto. Infine, si mescola il riempitivo secondo la percentuale di peso desiderata. Il composito viene lasciato riposare per almeno 15 minuti, al riparo dalla luce con un foglio di alluminio.

In questa relazione, il composito contenente il 56wt% di idrossiapatite (HA) come riempitivo è indicato come *formulazione prototipo*, essendo il materiale standard attualmente utilizzato nella tecnica AdhFix.

III. Risultati

III.i Tecnologia AdhFix attuale

La formulazione prototipo è stata sottoposta a uno screening delle proprietà meccaniche mediante prove di flessione a tre punti e la superficie di frattura è stata osservata con un microscopio a scansione elettronica (SEM) da banco per valutare eventuali relazioni microstruttura-proprietà meccaniche. La nomenclatura adottata in per i compositi usati in AdhFix è la seguente:

TIOLOxALCHENE (WT%)FILLER

A titolo di esempio, la formulazione prototipo di AdhFix, riportata nel paragrafo III, viene presentata come TMTATOxTATATO 56HA, dove TMTATO è il tiolo, TATATO l'alchene ed HA il riempitivo, in una concentrazione finale del 56% in peso. Il fotoiniziatore (TPO) e il catalizzatore sono presenti in proporzione costante con i monomeri. Per semplicità, nei grafici e nelle tabelle viene espresso solo il filler e la sua quantità, in quanto la matrice polimerica è sempre a base di TMTATOxTATATO.

Ogni nuovo lotto di TMTATO utilizzato per formulare il composito deve testato meccanicamente e confrontato con i risultati precedenti. I risultati delle prove di flessione a 3 punti (3PB) su due campioni del composito prototipo sono considerati accettabili e sono presentati in Tabella III.i.a insieme a quelli della pura matrice senza rinforzanti. I valori del sistema non caricato sono stati ottenuti dal collega D. J. Hutchinson.

Tabella III.i.a: Proprietà meccaniche di sistemi TMTATOxTATATO

Campioni	E_f [GPa]	σ_f [MPa]	Deformazione [mm/mm $\cdot 10^{-3}$]	Energia a rottura [mJ]
Matrice	2.9 (0.4)	99 (6)	96 (26)	95 (9)
56HA	6.6 (0.1)	59 (1)	9.6 (0.2)	11.4 (0.2)

Dopo le prove a flessione, la superficie di frattura di questi due campioni è stata osservata con un SEM da banco. L'immagine della superficie di frattura di uno dei campioni è presentata nella Figura III.i con basso (a, b x80) ed alto (c, x800) ingrandimento. Grazie all'uso di un software open source per l'analisi d'immagini (Fiji-ImageJ [76]), la porosità del composito TMTATOxTATATO 56HA è stata stimata al 20±5%. Sebbene i pori più piccoli siano stati osservati a ingrandimenti più elevati, il diametro minimo equivalente per

l'individuazione dei pori è stato fissato a 5 μm, poiché quelli più piccoli avrebbero richiesto un maggiore sforzo per distinguerli dalle cavità lasciate dal distacco o dal pull-out del riempitivo. L'intervallo di dimensioni dei pori è significativamente ampio, da 5 a oltre 450 μm di diametro proiezione. Si ritiene che una porosità così elevata influisca notevolmente sulle proprietà meccaniche del materiale, riducendo il volume di materiale che sostiene il carico.

La Figura III.i (c) mostra anche interessanti caratteristiche delle particelle di HA e delle sue interazioni con la matrice polimerica. L'HA appare come una particella secondaria, cioè un aggregato di cristalli di HA primaria, analogamente all'HA non sinterizzata [60,80], con una porosità intrinsecamente elevata. Ciò implica una superficie molto ruvida che potrebbe favorire l'adesione fisica con la matrice, ma potrebbe anche comportare una minor forza coesiva dell'aggregato stesso, non garantendo il rinforzo desiderato. Oltre alla presenza di porosità, è chiaramente visibile come le particelle di HA non abbiano una buona adesione alla matrice polimerica, con uno spazio visibile tra questi ed un esteso distacco delle particelle piuttosto che un loro cedimento coesivo durante la frattura. Nel caso dei compositi rinforzati con particelle (PRC), come nel caso della formulazione prototipo di AdhFix, il pull-out non è un meccanismo di rinforzo significativo, poiché la forma sferica non consente l'attrito dissipativo con la matrice. È invece generalmente preferibile massimizzare l'adesione interfacciale per migliorare il modulo e la resistenza del materiale. [31]

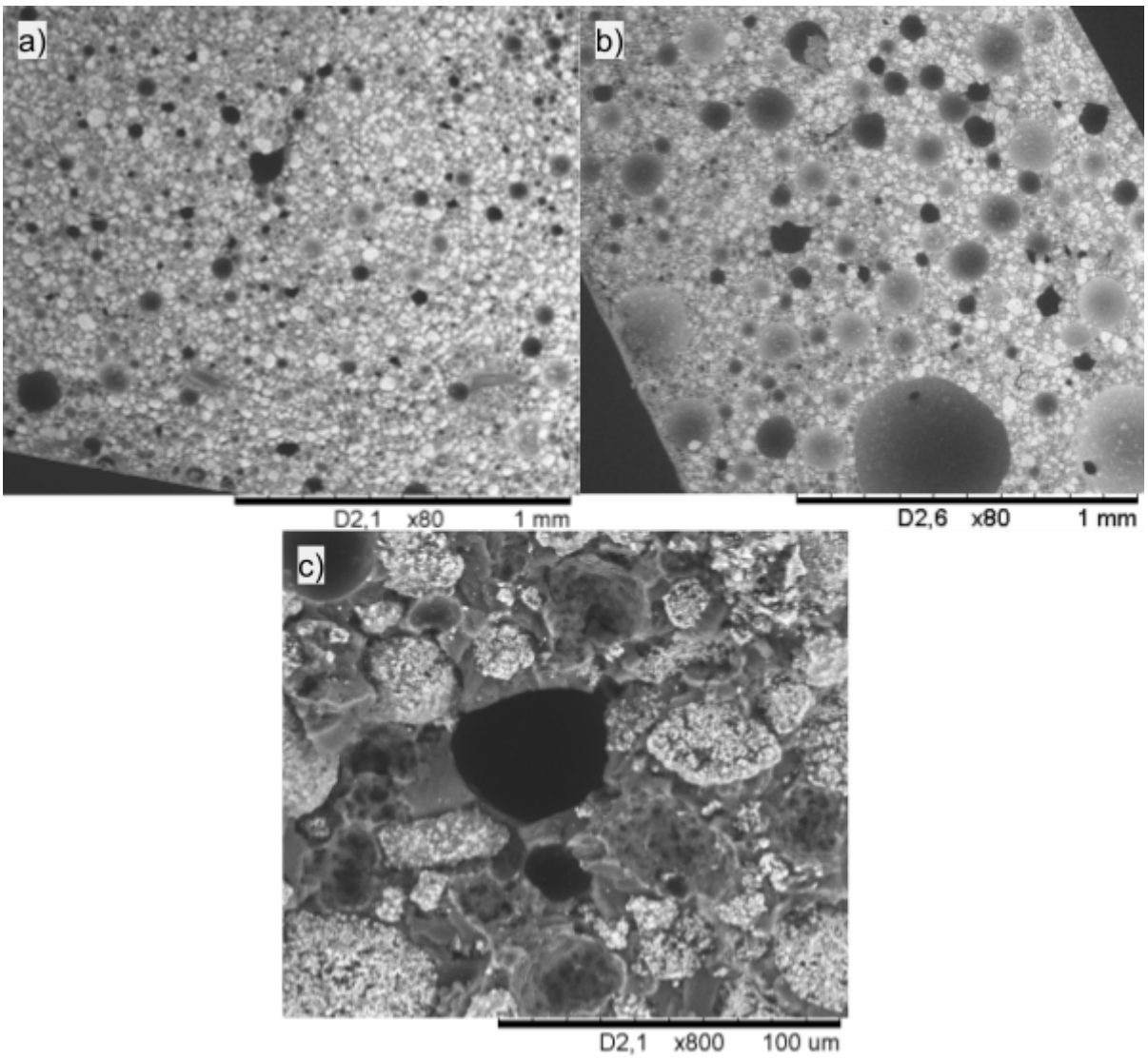

Figura III.i*: Superfici di frattura di TMTATOxTATATO 56HA a 80x (a,b) e 800x (c)*

La formulazione prototipo è stata utilizzata per testare la fattibilità della produzione di viti e le potenziali criticità del processo per diversi diametri di vite. Sono state realizzate viti di diverso diametro sia con il composito 56HA che con il termoindurente puro TMTATOxTATATO. Sono state poi avvitate e svitate (quando possibile) in un metacarpo suino precedentemente maschiato con una vite in acciaio della stessa geometria. La Tabella III.i.b mostra il numero di viti inserite con successo (✅) o rotte (❌) per i diversi diametri nominali delle viti; ogni segno di spunta o croce rappresenta una vite. Sebbene questi risultati presentino una scarsa significatività statistica, confermano che l'attuale formulazione è inaccettabile per viti con piccoli diametri e suggeriscono, come atteso, che le viti più grandi non richiedono proprietà meccaniche specifiche così elevate per essere utilizzate con successo.

La maggior parte delle criticità riscontrate riguarda la presenza di bolle o problemi con l'intaglio. La maggioranza delle viti si è fratturata in corrispondenza del collo e ha presentato lungo la superficie di frattura una o più bolle visibili ad occhio nudo. Queste cavità probabilmente sono riconducibili a quelle già presenti nel composito come osservato in precedenza. Sono state osservate cavità anche in due casi in cui le viti si sono fratturate nel

gambo applicando solo una minima torsione. Nel caso di campioni più grandi, come quelli sottoposti a flessione a 3 punti o le patch per fissaggio di fratture ossee (BFPs) utilizzate da Hutchinson et al. [3], la presenza di porosità può influire sulle proprietà meccaniche ma non è così critica, in quanto si possono comunque ottenere risultati soddisfacenti. Nel caso delle viti, invece, la presenza di porosità residua appare inaccettabile e particolarmente dannosa per le viti di diametro inferiore, poiché una singola cavità può ridurre significativamente l'area di resistenza lungo il gambo o nel collo, portando ad una frattura prematura.

Anche gli intagli decentrati sembrano causare alcuni problemi: l'impossibilità di imprimerli perfettamente lungo l'asse della vite provoca, durante l'inserimento, un aumento di sollecitazioni complesse che potrebbe contribuire ulteriormente a rotture premature. Si conclude che per viti corticali sono necessarie proprietà meccaniche più elevate.

Tabella III.i.b: Risultati dell'inserzione di viti in sola matrice di TMTATOxTATAO o in composito con 56HA in metacarpi suini precedentemente maschiati

Diametro [mm]	2.0	2.5	3.5	4.0
56HA	❌❌❌❌	✅❌❌❌❌	❌✅	✅
Solo matrice	❌❌❌❌	✅✅❌	✅✅	✅

III.ii Screening di diversi rinforzanti (filler)

In un primo tentativo di migliorare le proprietà meccaniche del composito, l'HA è stata sostituita con altri riempitivi: vetro bioattivo 58S (Bgl), whisker di idrossiapatite (HA-w) e una polvere apatitica nota come "MCD abrasivo apatitico" [81]. L'MCD è stato scelto perché è un materiale apatitico sinterizzato, quindi con proprietà meccaniche superiori all'HA porosa, presumibilmente non sinterizzata. Gli HA-w (modulo elastico 70-140 GPa [82,83]) è stato scelto con un ragionamento simile, ma con l'aggiunta del fatto che le particelle con aspect ratio più elevato sono note per essere agenti di rinforzo più efficaci, grazie all'aumento del trasferimento delle sollecitazioni di taglio e flessione e alla maggiore area superficiale specifica [31]. Il Bgl, invece, è stato scelto per introdurre una componente riassorbibile nella formulazione del composito, in vista di un sistema completamente riassorbibile. Il vetro bioattivo è ampiamente studiato in campi come l'odontoiatria e specialmente nella medicina rigenerativa grazie alle sue proprietà osteoinduttive [84].

In primo luogo, è stata valutata la quantità massima di riempitivo che la resina TMTATOxTATATO poteva incorporare. Questa è stata definita come la frazione in peso di riempitivo che può essere aggiunta ai monomeri per ottenere la stessa viscosità pre-polimerizzazione dela formulazione prototipo; ed è stata determinata essere 36, 58 e 62 wt.% rispettivamente per Bgl, HA-w e MCD. La determinazione della viscosità è stata eseguita visivamente.

Le proprietà meccaniche dei compositi con la massima quantità di riempitivo sono presentate in Tabella III.ii. Il riempitivo più promettente appere essere HA-w, con un aumento di modulo e di resistenza a flessione rispettivamente del 37% e del 20% rispetto al composito prototipo. La formulazione con abrasivo apatitico sinterizzato, invece, ha mostrato le peggiori prestazioni di resistenza, in quanto l'aumento del carico di particellare prive di adesione interfacciale diminuisce l'area di resistenza[32,38]. La formulazione con bioglass

ha mostrato il modulo più basso, come atteso, considerato che la frazione volumetrica ed il suo modulo sono significativamente inferiori rispetto alle cariche apatitiche.

Tabella III.ii*: Proprietà mecchaniche di TMTATOxTATATO a massimo carico di diversi filler*

Campioni	E_f [GPa]	σ_f [MPa]	Deformazione [mm/mm $\cdot 10^{-3}$]	Energia a rottura [mJ]
56HA - prototipo	6.6 (0.1)	59 (1)	9.6 (0.2)	11.4 (0.2)
36 Bgl	4.5 (0.3)	50 (3)	11.5 (0.4)	11.5 (0.9)
58 HA-w	9.1 (0.2)	71 (3)	9.6 (0.5)	11.8 (1.1)
62 MCD	5.5 (0.3)	43 (2)	11.0 (0.1)	11.0 (0.1)

Per correlare tali risultati alla microstruttura del composito, le superfici di frattura sono state osservate con un SEM da banco. La Figura III.ii presenta alcune micrografie delle superfici di frattura del composito con MCD (a), Bgl (b) e HA-w (c,d). La distanza tra le particelle di MCD e la matrice mostra inequivocabilmente l'assenza di adesione tra i due componenti. Il motivo principale per cui la formulazione prototipo dà luogo a a proprietà migliori rispetto a quella con MCD è probabilmente riconducibile all'adesione fisica ed incastro tra matrice e particelle, che appare svolgere un ruolo significativo quando si utilizzano particelle porose come HA, ma è escluso quando si utilizzano particelle dense e lisce come MCD. Poiché l'MCD presenta le peggiori proprietà meccaniche e non è riassorbibile, è stato escluso da ulteriori indagini.

L'interfaccia HA-w polimero mostrata nella Figura III.ii (d) appare scarsa tanto quanto quella dell'HA e dell'MCD. È dunque improbabile che l'adesione interfacciale sia un fattore che contribuisce alle migliori proprietà della formulazione con HA-w. Una spiegazione ragionevole risiede nella meccanica geometrica del sistema con particelle rigide ad alto aspect ratio come HA-w: poiché l'HA-w ha un modulo elastico di circa due ordini di grandezza superiore a quello della matrice polimerica, possono essere considerati come barre indeformabili immerse in una matrice deformabile. Quando al composito viene applicato un carico, la matrice si deforma, seppur leggermente, e, grazie all'elevato rapporto d'aspetto dei whisker, forma punti di contatto con questi ultimi, attraverso i quali avviene un trasferimento degli sforzi. Poiché i whisker non sono orientati in modo preferenziale, questo fenomeno può verificarsi indipendentemente dalla modalità di applicazione del carico, garantendo un rinforzo isotropico.

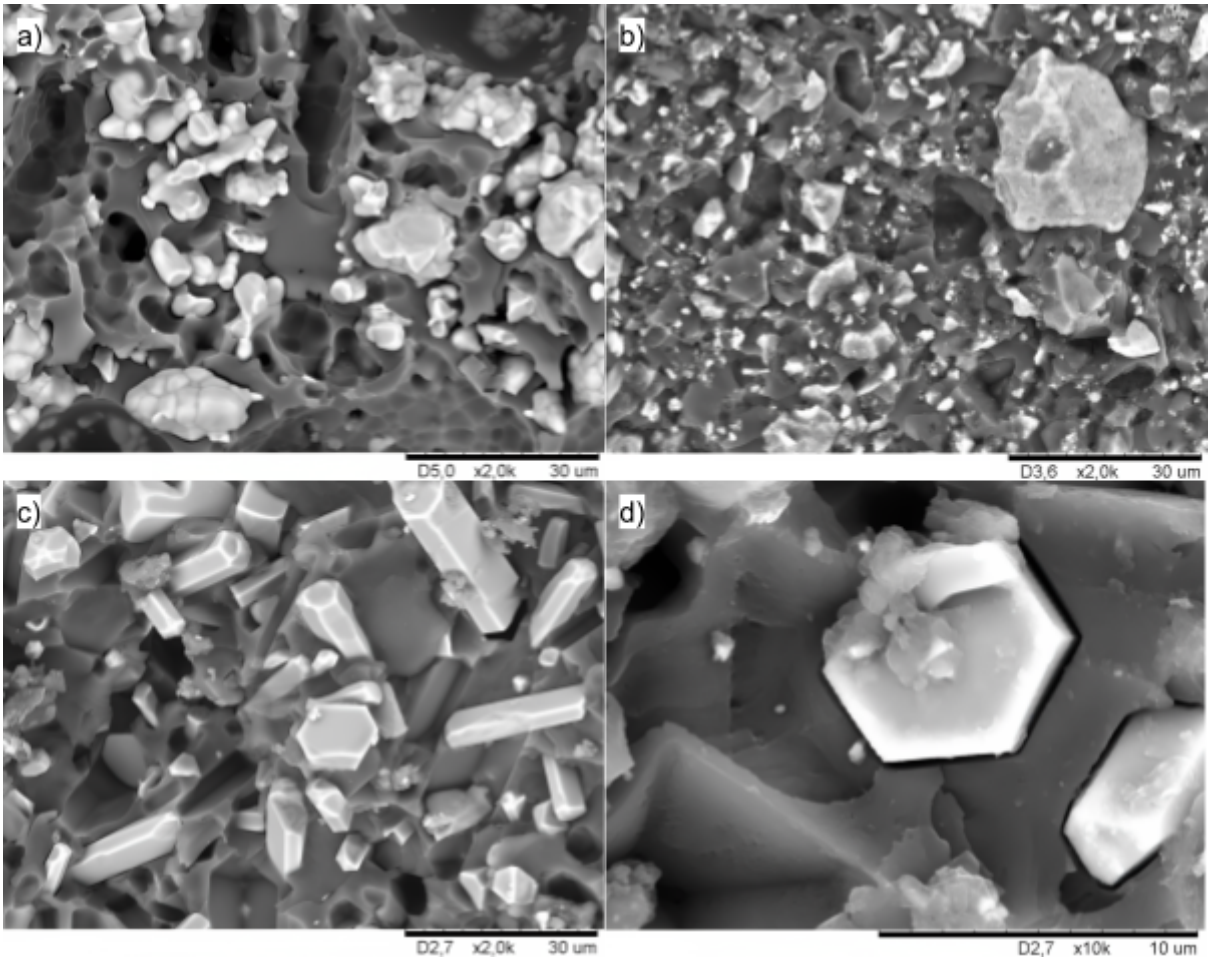

Figura III.ii*: Micrografie SEM di compositi a matrice TMTATOxTATATO con diversi rinforzanti: MCD (a x2000), Bgl (b x2000), HA-w (c x2000, d x10000)*

III.iii Degasaggio dei compositi a matrice tiolo-enica

Come strategia per ridurre la porosità del materiale prima della polimerizzazione, una fase di degasaggio è sembrata la più facilmente applicabile su scala di laboratorio, senza bisogno di attrezzature ad hoc. Dopo la miscelazione dei componenti e del riempitivo, il composito è stato quindi posto sotto vuoto in linea Schlenk per 1,5 ore .ca, dopodiché è stato formato e polimerizzato. I risultati dei test a flessione per i compositi degasati con 58HA-w e 56HA sono presentati nella Tabella *III.iii*, a confronto con le loro controparti non degasate. In entrambi i casi, il degasaggio ha permesso di ottenere proprietà meccaniche superiori ed è stato quindi aggiunto alla procedura standard di produzione dei compositi.

Tabella III.iii: Proprietà meccaniche di compositi a matrice TMTATOxTATATO con e senza un processo di degasaggio in vuoto

Campioni	E_f [GPa]	σ_f [MPa]	Deformazione [mm/mm $\cdot 10^{-3}$]	Energia a rottura [mJ]
56HA	6.6 (0.1)	59 (1)	9.6 (0.2)	12 (2)
56HA degas	7.5 (0.5)	58 (5)	9.0 (0.4)	9 (1)

58 HA-w	9.1 (0.2)	71 (3)	9.6 (0.5)	12 (1)
58 HA-w degas	9.4 (0.3)	81 (5)	10.2 (0.5)	15 (2)

È interessante notare, tuttavia, che la variazione delle proprietà meccaniche sembra essere diversa tra le formulazioni con HA e HA-w. Mentre i campioni con 56 HA hanno mostrato un aumento del modulo a flessione (.ca 14%), ma non della resistenza alla flessione, l'opposto si è verificato per i campioni con 58HA-w, dove la resistenza a flessione è aumentata di .ca 14%, ma non sono state osservate variazioni significative del modulo. Una possibile spiegazione di questo fenomeno risiede ancora una volta nelle differenze strutturali dei riempitivi. Poiché l'HA è porosa, quando si applica il vuoto, la penetrazione della matrice all'interno dei pori viene favorita, aumetando l'adesione fisica tra le due fasi. La mancanza di un aumento della resistenza può essere attribuita alla limitata forza coesiva degli aggregati, che potrebbe o essere il fattore limitante della resistenza o fornire punti di concentrazione degli sforzi.

Gli HA-w invece, non essendo porosi, non possono beneficiare del'adesione fisica alla matrice polimerica. Il vuoto potrebbe ridurre lo spazio tra la matrice e i whisker, migliorando il trasferimento degli sforzi, che, combinato con una riduzione complessiva della porosità, potrebbe spiegare l'aumento della resistenza. Si ritiene comunque che il principale meccanismo sia la riduzione della porosità, e di conseguenza l'aumento dell'area resistente, ma sono necessarie ulteriori indagini per chiarire il punto.

La riduzione della porosità può essere chiaramente apprezzata in Figura *III.iii*, dove le superfici di frattura dei compositi non trattati con 58HA-w (a,b) sono confrontate con la loro controparte degasata (c).

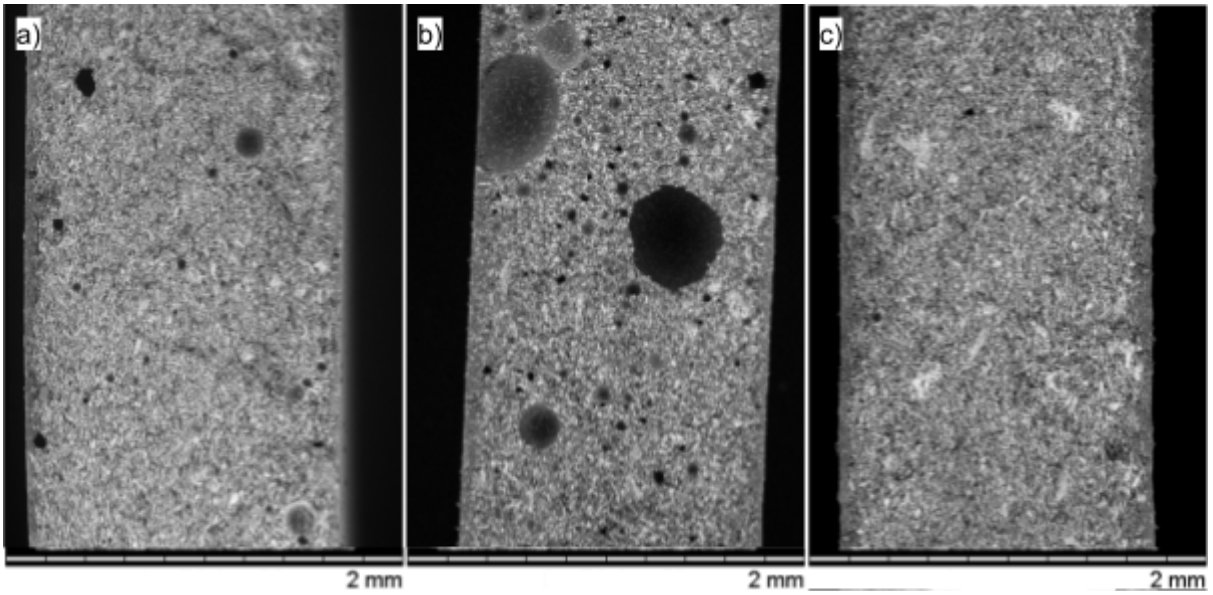

Figura III.iii: Superfici di frattura di TMTATOxTATATO 58HA-w senza (a: miglior campione, b peggior campione) e con (c) il processo di degasaggio in vuoto

III.iv Funzionalizzazione dei rinforzanti

Seguendo la logica introdotta in precedenza, sono stati scelti due diversi riempitivi per studiare l'effetto della loro funzionalizzazione sulle proprietà meccaniche del composito polimerizzato. HA-w e Bgls sono stati scelti come candidati promettenti rispettivamente per le loro proprietà meccaniche o di riassorbibilità. La Figura *III.iv* mostra le molecole scelte come agenti di compatibilizzazione per i riempitivi utilizzati. Il Bgl è stato silanizzato con γ-MPS, in quanto già abitualmente impiegato per la silanizzazione della silice nei compositi dentali e presenta tra le più alte proprietà di rinforzo [43]. Inoltre, la coda metacrilica fornisce un doppio legame C-C che può copolimerizzare con il TMTATO durante la fase di fotoindurimento, legando covalentemente le particelle di Bgl alla matrice polimerica.

Gli HA-w, invece, sono stati funzionalizzati con due diversi acidi fosfonici non commercialmente disponibili, PEMPA e UEMPA. Gli acidi fosfonici sono stati scelti rispetto agli organosilani perché, rispetto a questi ultimi, formano un legame più stabile con gli ossidi non a base di silice [50,51]. Il gruppo vinilico terminale è stato selezionato, per consentirne la copolimerizzazione con la matrice, analogamente al γ-MPS. Sono state selezionate anche diverse lunghezze delle code insature, poiché questo era ritenuto un parametro che ne influenza l'affinità verso la matrice, dunque, la loro efficacia compatibilizzante.

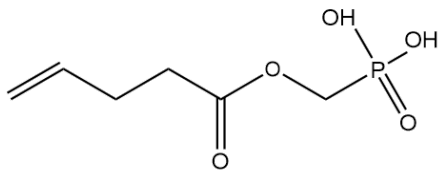

((pent-4-enoyloxy)methyl)phosphonic acid (PEMPA)

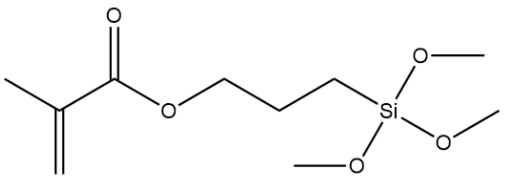

γ-methacryloxypropyltrimethoxysilane (γ-MPS)

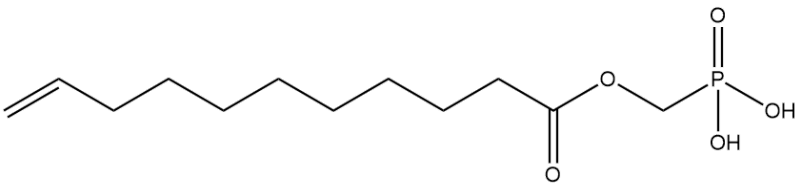

((undec-10-enoyloxy)methyl)phosphonic acid (UEMPA)

Figura III.iv: molecole compatibilizzanti usate in questo progetto

Sono state prodotti campioni di composito con il 58wt% di HA-w funzionalizzati con PEMPA e UEMPA, nonché con il 36wt% di Bgl funzionalizzato con γ-MPS. Tutti i compositi sono stati sottoposti alla procedura di degasaggio. I risultati delle prove di flessione a tre punti sono presentati nella Tabella *III.iv*, a confronto con le loro controparti degassate non funzionalizzate.

I compositi con HA-w funzionalizzato non hanno mostrato un miglioramento delle proprietà meccaniche. Anzi, sorprendentemente, sembrano mostrare un modulo di flessione

leggermente inferiore, significativo solo per l'UEMPA, mentre tutte le altre proprietà rimangono invariate. Le cause di questo effetto negativo non sono state indagate per motivi di tempo, ma potrebbero essere simili a quelle riscontrate da Altan et al. [85], dove alcuni compatibilizzanti hanno portato all'aggregazione delle particelle e a una dispersione meno efficiente. Altre possibilità potrebbero includere una scarsa interazione tra i compatibilizzanti ed il TMTATO, ostacolandone la copolimerizzazione.

D'altra parte, il composito con Bgl silanizzato ha mostrato notevoli miglioramenti di tutte le proprietà meccaniche. L'aumento del modulo essendo il più modesto, pari solo al 20%, la resistenza alla flessione è aumentata del 120%, la deformazione a rottura del 160% e l'energia a rottura del 500% circa. L'energia a rottura è un parametro particolarmente importante, poiché è strettamente legato alla resistenza agli urti e alla fragilità di un materiale. Sebbene non si preveda che le viti per fissazione ossea subiscano impatti significativi dopo l'impianto, un'elevata tenacità facilita notevolmente la manipolazione da parte del chirurgo, riducendo il rischio di rotture indesiderate. Confrontandola con la formulazione con HA-w, presenta solo circa il 60% del suo modulo, ma la resistenza e l'energia a rottura aumentano rispettivamente del 40% e del 400%.

Osservazioni al SEM delle superfici di frattura sarebbero state auspicabili, ma non sono state possibili a causa di un guasto allo strumento e dei limiti di tempo.

Tabella III.iv: Proprietà mecchaniche di compositi degasati a matrice TMTATOxTATATO con rinforzanti funzionalizzati o meno.

Campioni	E_f [GPa]	σ_f [MPa]	Deformazione [mm/mm $\cdot 10^{-3}$]	Energia a rottura [mJ]
36Bgl-no degas	4.5 (0.3)	50 (3)	11.5 (0.4)	11.5 (0.9)
36Bgl+γ-MPS	5.4 (0.1)	111 (8)	30 (0.4)	73(28)
58HA-w	9.4 (0.3)	81 (5)	10.2 (0.5)	15 (2)
58HA-w+PEMPA	8.5 (0.6)	81 (6)	10.3 (0.6)	15 (2)
58HA-w+UEMPA	8.1 (0.3)	79 (3)	10.7 (0.9)	16 (2)

III.v Confronto di proprietà meccaniche

L'aggiunta della degassificazione, così come l'introduzione di Bgl silanizzato o HA-w, ha esteso il confine delle proprietà meccaniche delle formulazioni AdhFix, aumentando rispettivamente la tenacità e la resistenza o il modulo elastico. La Figura III.v presenta un diagramma di Ashby resistenza-modulo a flessione delle formulazioni AdhFix contenenti 56HA con o senza degasaggio, 36BGL non degasato, 36BGL+γ-MPS degasato, 58HA-w degasato. Sono inclusi anche i valori di un polimero tiolo-enico non caricato sviluppato in precedenza [20], di polimeri disponibili in commercio, ovvero PLA e un composito di fibre PLA/PGA 70:30 [90], nonché di PEEK [91]. I valori del più forte composito riassorbibile conosciuto (utilizzato per SuperFIXSORB-MX®) non sono inclusi in quanto fuori dai valori

degli assi, ma sono riportati nella tesi in sezione 2.2.3 con modulo di flessione e resistenza rispettivamente di 12 GPa e 270 MPa [53].

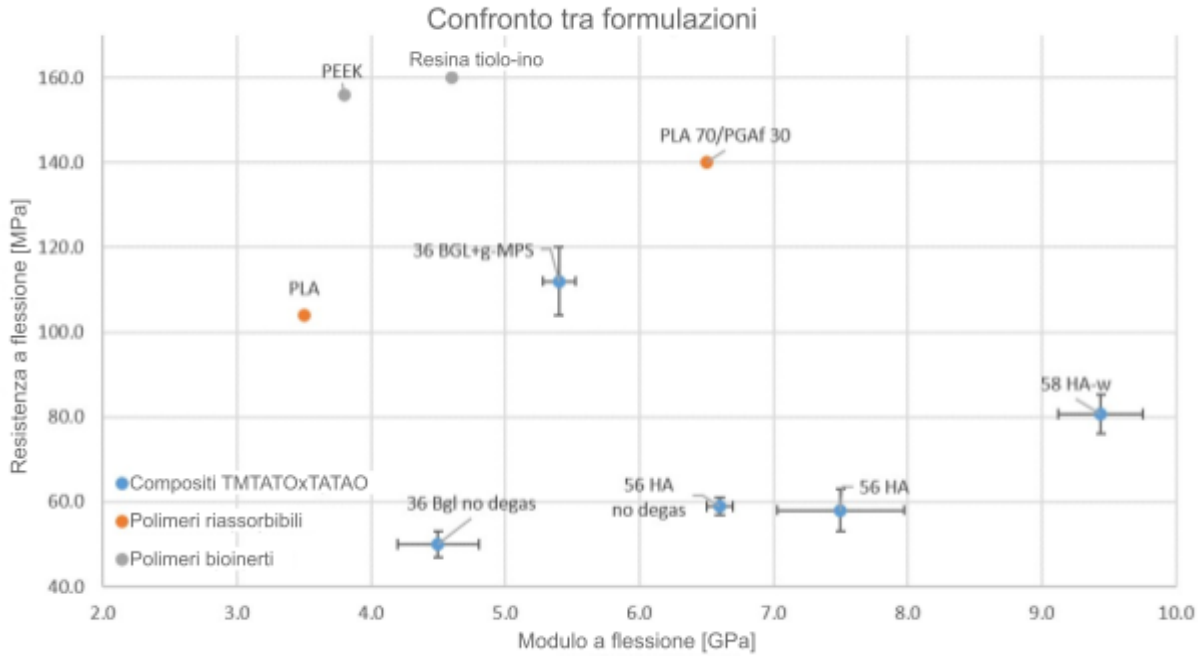

Figura III.v*: Proprietà meccaniche di diverse formulazioni AdhFix, resina tiolo-ino, e materiali polimerici biomedicali commercialmente disponibili*

III.vi Fissazione di fratture modello

Viti bicorticali in materiale composito sono state prodotte con diametri (∅) di 1.5 e 2.5 mm utilizzando TMTATOxTATATO 36Bgls+γ-MPS. Questa formulazione è stata scelta in quanto presentava la massima resistenza a flessione ed energia a rottura, riducendo così il rischio di rottura accidentale dovuta a una manipolazione errata durante l'inserimento. Sono state quindi utilizzate al posto delle viti metalliche per la procedura AdhFix su fratture trasversali modello su metacarpi suini. Qualitativamente, la differenza rispetto alle viti prototipo presentate in Tabella III.i.a è evidente, poiché delle quattordici viti da ∅1.5 mm contenenti 36Bgl+γ-MPS, solo due si sono rotte durante l'inserimento, rispetto alla totalità delle viti con 56HA da ∅2 mm di cui alla Tabella III.i.a. Di queste due, una presentava un'ampia cavità nel gambo, sulla superficie di frattura, mentre l'altra si è rotta a causa di una manipolazione errata dovuta all'applicazione di una sollecitazione di taglio tramite un movimento involontario della mano. Sebbene questi risultati mostrino un grande miglioramento rispetto alla formulazione convenzionale, la sensibilità di queste viti ai carichi involontari rappresenta uno svantaggio importante per una futura applicazione clinica. L'aumento delle dimensioni delle viti a solo ∅2.5 mm, tuttavia, conferisce loro una resistenza e proprietà meccaniche di gran lunga superiori, suggerendo che il loro utilizzo potrebbe essere preso in considerazione per fratture più grandi.
La Figura III.vi (sx) presenta i risultati a flessione di fratture metacarpali suine con BFPs di TMTATOxTATATO 36Bgl+γ-MPS e fissate alle ossa con viti composite ∅1.5 mm e ∅2.5 mm, o con viti metalliche (Ti6Al4V) ∅1.5 mm, rispettivamente la prima, seconda e terza colonna da sinistra. La quarta colonna rappresenta la tecnologia attuale, ovvero BFPs prodotte con la formulazione prototipo di AdhFix ed fissate con viti ∅1.5 mm metalliche. A destra (dx), i

risultati sono normalizzati rispetto alla superficie delle fratture per ottenere valori che tengano conto, anche se in maniera molto approssimativa, dello spessore del patch.

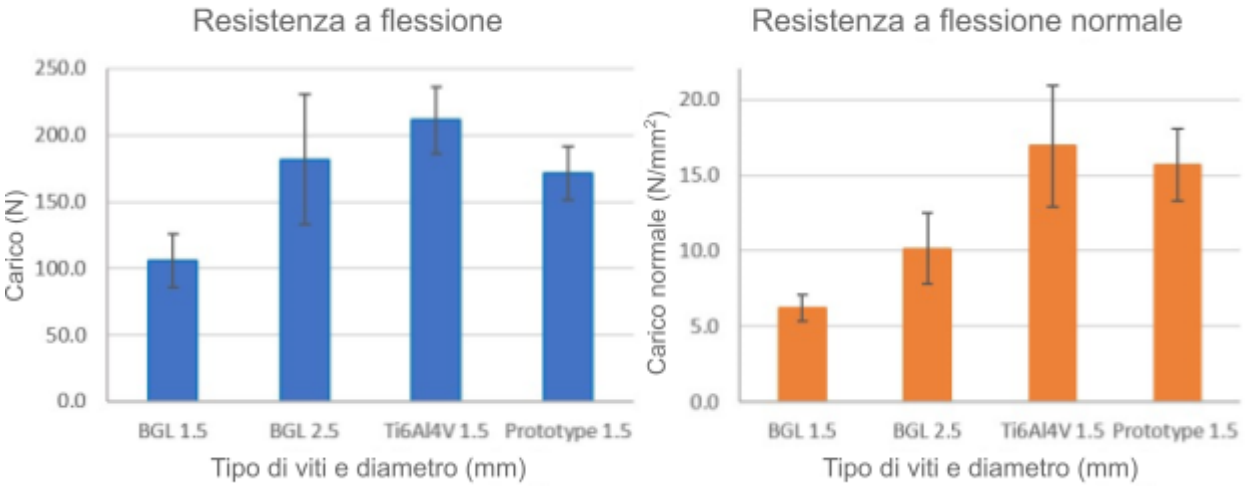

Figura III.vi*: resistenza a flessione di BFPs di* TMTATOxTATATO *36BGL*+γ-MPS *(sx) e resistenza a flessione normalizzata (dx) con diverse viti (da sinistra a destra: ∅1.5 e ∅2.5 mm in composito, ∅1.5 mm metal) confrontati con i BFPs di formulazione prototipo con viti ∅1.5 mm metalliche.*

Questi risultati mostrano chiaramente che la resistenza dei BFPs completamente in composito è limitata dalle dimensioni delle viti. I BFPs con viti da ∅2.5 mm hanno mostrato un aumento significativo della resistenza, raggiungendo risultati paragonabili a quelli ottenuti con viti metalliche. La resistenza normalizzata sembra confermare questa tendenza, sebbene sia evidente una maggiore differenza tra i BFPs con viti metalliche e quelli con viti composite da ∅2.5 mm. Il fatto che le viti da ∅1.5 mm siano il fattore limitante della resistenza è ulteriormente supportato dal fatto che durante i test, la rottura è avvenuta al collo delle viti, con conseguente distacco del BFP. Al contrario, quelle in composito da ∅2.5 mm, hanno subito la frattura del patch stesso. In quest'ultimo caso, la frattura ha riguardato l'interfase patch-testa di vite, come nel caso delle viti metalliche, suggerendo che tale regione offre una resistenza inferiore rispetto al patch massivo o agisce come regione di concentrazione degli sforzi.

Sebbene i sistemi completamente compositi appaiano meno resistenti dei BFPs prototipo, i BFPs realizzati con la nuova formulazione 36BGL+γ-MPS mostrano una resistenza comparabile o superiore nonostante l'introduzione di componenti riassorbibili. Inoltre, pur avendo la minor resistenza tra quelli analizzati, i BFPs completamente in composito con viti da ∅1.5 mm sono meccanicamente equivalenti, se non superiori, alla resistenza dei K-wire, che cedono dopo 80 (6) N [3].

IV. Conclusioni

Poiché l'attuale formulazione del prototipo AdhFix non possiede proprietà meccaniche soddisfacenti per la produzione di viti di piccole dimensioni, sono state studiate tre diverse

strade per risolvere il problema: la sostituzione del riempitivo, l'aggiunta di una fase di degasaggio e la funzionalizzazione dei riempitivi con compatibilizzanti con un gruppo allilico.

La sostituzione delle particelle porose di HA con whisker di idrossiapatite (HA-w) ha mostrato il maggior miglioramento tra i riempitivi esaminati, aumentando la resistenza ed il modulo a flessione rispettivamente del 20% e del 37%. Tutti i riempitivi hanno mostrato una scarsa adesione con la matrice di TMTATOxTATATO, ma la struttura porosa dell'HA può dare origine aadesione fisica, mentre l'elevato aspect ratio dei HA-w ha garantito più punti di contatto. La formulazione con BGL non funzionalizzato ha avuto il modulo più basso a causa della minor frazione di rinforzanti.

L'aggiunta di un degasaggio in vuoto ha ridotto significativamente la porosità del materiale, ma gli effetti sulle proprietà meccaniche finali appaiono dipendere dalla morfologia del riempitivo e non sono universali. Per i riempitivi densi e non porosi, l'effetto appare essere un aumento dell'area resistente, che a sua volta migliora la resistenza del materiale. Per filler porosi, l’applicazione di vuoto potrebbe inoltre promuovere l'incastro meccanico, favorendo il trasferimento delle sollecitazioni.

La funzionalizzazione dei filler ha dato risultati contrastanti. Il BGL funzionalizzato con γ-MPS e degassato ha migliorato notevolmente le proprietà meccaniche del composito, con un aumento del 120% della resistenza alla flessione e del 500% dell'energia a rottura. D'altra parte, i HA-w funzionalizzati con acidi fosfonici non hanno mostrato alcun miglioramento nelle capacità di rinforzo. Le cause di questo effetto non sono state investigate in questo progetto, anche se si ipotizza che possano essere legate a una bassa area superficiale specifica, a una funzionalizzazione incompleta o a un'interazione inadeguata tra il compatibilizzante e la matrice polimerica.

Infine, sono state prodotte viti di ∅1.5 e 2.5 mm in TMTATxTATATO 36BGL+γ-MPS per testare patch di fissazione ossea completamente compositi. La loro resistenza è risultata limitata dalle viti quando sono state utilizzate quelle da ∅1.5 mm, sebbene superassero comunque la resistenza allo snervamento dei K-wire. I BFPs completamente compositi con viti da ∅2.5 mm hanno mostrato una resistenza paragonabile, se non superiore, ai BFPs realizzati con la formulazione prototipo con viti metalliche. Nel complesso, è stato dimostrato che è possibile ottenere un sistema di fissazione ossea completamente composito e personalizzabile basato su compositi a matrice tiolo-ene. Inoltre, l'introduzione di fasi riassorbibili non ha compromesso la resistenza dei BFPs.

Thesis

1. Introduction

Bone fractures are common injuries caused by medical conditions or accidents, which range from minor bone fissures to major damage which leads to intense pain and can cause permanent damage and mobility issues. Bone fracture occurrences have been increasing in the past decades, reaching nearly 180 million in 2019, and are expected to keep growing, pushed by the growth in population and its increase in age[1]. In the case of a simple fracture, it is generally sufficient to immobilise the bone with an external device such as a cast or splint. In the case of more complex fractures or where external immobilisation is not effective, surgery is required to fix the bone. The current standard of care for open reduction internal fixation (ORIF) surgery employs metal devices such as pins, wires, plates and screws to secure the bones in place and allow for healing. However, they suffer from various limitations such as poor customizability, stress shielding, and soft tissue adhesion which can lead to impaired mobility[2].

The group of professor Malkoch in the Division of Coating Technology at KTH Royal Institute of Technology is developing thiol-ene (TE) based systems for the fixation of fractured bones. Namely, a methodology called AdhFix currently employs an in-situ photocurable composite anchored to bone with metallic cortical screws as a substitute of rigid plate and screws fixation[3]. This grants surgeons an unparalleled possibility of shaping the fixator to the patients' needs.The ultimate goal is to develop a fully resorbable fixation system, where metal screws are replaced by polymeric matrices. This approach aims for a non-metallic fixation system that can be tweaked to introduce resorption properties. With the current composite composition (comprising TMTATO as thiol, TATATO as alkene and 56 wt% hydroxyapatite as filler), however, attempts to produce smaller screws (i.e. up to 2.5 mm in diameter) have resulted in unacceptable performance, with screw failure during insertion into bone.

Building upon the current AdhFix technology, the aim of this project is to replace metal screws with TE-based composite screws as a first step towards complete resorbability. To achieve this, new formulations with improved mechanical properties were developed, including bioresorbable components. The workload has been structured around three branches:

1. Introduction of fillers granting superior mechanics or resorbability
2. Reduction of the material's porosity
3. Surface functionalization of fillers for improved compatibility

2. Background

2.1 Bone fracture fixation and hand fractures

The first use of metal devices for bone fracture fixation was reported as early as the end of the 18th century [4]. Since then, research in surgery and materials science has led to tremendous improvements in the surgical techniques and alloys' properties. Pins, wires, plates and screws are nowadays available in a wide range of designs and alloys, generally titanium- or stainless steel- based , each most suitable for specific applications. As a matter of fact, metallic implants are the gold standard when it comes to unsteady bone fractures that require surgery and internal fixation. Despite the outstanding advancements and widespread use, these devices are not exempt from complications, which vary depending on the application.

The most common drawbacks of metallic implants fall within the category of foreign body reactions (FBRs). FBR is initiated by the competitive adsorption and denaturation of proteins on the surface of the material, which initiate a signalling cascade that leads to an immune response, inflammation, granuloma formation, and eventually fibrous encapsulation [5]. FBR is modulated by a variety of different factors such as the surface's chemical properties, its roughness, the overall tribology, the implant geometry and its mechanical properties [6]. In the most severe situations, this can lead to severe pain, chronic inflammation, or even the need for reoperation with permanent damage to the area. Local damage can also be caused by the release of metal ions or particles as a consequence of unwanted localised wear or oxidation. [7,8]

Commercially available metal devices have a much higher modulus of elasticity compared to the bone (e.g. Ti6Al4V 116 GPa against 5-23 GPa for cortical bone). This leads, especially in load bearing positions, to most of the load being carried by the implant, a situation named "stress shielding" which in turn causes a reduction in the surrounding bone density (osteopenia)[9,10] . From a surgical perspective, the major drawback is that metal plates are inherently not customizable during the surgery due to their stiffness, preventing an effective use with smaller or non-flat bone segments.

Fractures of phalangeal or metacarpal bones are amongst the most common fractures to occur, and are the most common in the 18-35 years old range in the United States of America, accounting for over 50% of all fractures in this age group [11]. In 1996, in the Accident and Emergency Department of the VU University Medical Centre in Amsterdam,

fractures to phalanges or metacarpals accounted for 19% of the total fracture cases [12]. Furthermore, these fractures expose patients to a high risk of postoperative complications. These occurrences are reported in different ranges, depending on the complexity of the fracture, type of fixation, considered cohort, etc. The overall order of magnitude however lays around 30-50% of major complications, rising over 60% when considering phalangeal fractures fixated with metal plates [2,13]. The most common complications include stiffness, complex regional pain syndrome, infection, delayed union, nonunion, malunion, and plate loosening [13,14]. These issues often lead to the need for reoperation, up to 42% for the phalanges fractures treated with plate fixation [15].

2.1.1 Kirschner wires (K-wires)

Kirschner wires, shortened to K-wires, are sharpened stainless steel pins that are commonly, but not exclusively, employed as fixators in hand fractures. Their use generally involves an x-ray guided insertion through the skin and into the bone fragments that require to be kept aligned. Various geometries and configurations, with single or multiple wires, can be used depending on the case and the surgeons' judgement. K-wires have many positive aspects: the procedure is generally short and percutaneous insertion, rather than open reduction, limits the damage to the surrounding soft tissue; removal is fast and easy as part of the k-wire is external; finally they are cheap. On the other hand, k-wires are generally only able to keep the bone alignment but not to maintain compression between them and cannot withstand flexural stresses. For this reason, they generally need additional external immobilisation such as a cast or splint; which doesn't allow for significantly early stage mobilisation, substantially increasing the risk of tendon adhesion and future mobility reduction. Other issues include pin migration causing malunions, pin tract infection, and, occasionally, complex regional pain syndrome. [16,17]

2.1.2 Open Reduction Internal Fixation (ORIF)

ORIF in hand fractures generally involves the use of metal plates and screws to fix bone pieces in position. For phalangeal and metacarpal fractures, the surgery is performed from the dorsal side due to ease of access to the bones, decreasing the extensive soft tissue damage that would follow a palmar approach. This allows for a very limited thickness of the plate, as the friction exerted on the extensor tendons can impair gliding, leading to irritation or bursal formation[18]. This has led to the development of plates with a lower profile (1.1-1.3 mm) than the conventional 2.7 mm dynamic compression plate, suitable for particular conditions[19,20]. Other drawbacks of plate systems are related to FBR and soft tissue adhesion which hinder mobility recovery, and to soft tissue damage caused by bicortical screws protruding from the bone, which can lead to tensor tendon damage or

rupture[21]. For these reasons, plate systems generally undergo a second surgery for removal after the fracture's healing. The high mechanical properties of plate and screw systems, however, allow for a more secure fixation that is able to support normal bending stresses, allowing for early mobilisation of the joints, which is considered a crucial parameter for maximum mobility recovery.

2.2 Polymer-based materials in bone fixation

Presently, most bone fracture fixation systems are made from various grades of stainless steel or titanium alloys due to their satisfactory biocompatibility and superior mechanical properties. However, because of the previously mentioned limitations, a wide range of polymer-based materials, bioresorbable or bioinert, have emerged in recent decades. Currently, a wide range of properties can be achieved by combining, tweaking and optimising the processing of just a handful of materials. The most common polymers and reinforcing agents for bone fixation applications are presented in the following paragraphs.

2.2.1 Common biomedical polymers for bone fixation

Polylactic Acid (PLA) is among the most widely used resorbable polymers in bone fixation. It can be derived from renewable resources and among its advantages, its degradation yields lactic acid which can be metabolised by the body. PLA can arrange into highly crystalline structures, significantly affecting its mechanical and degradation properties. Its ultimate tensile strength (UTS) can range from 16 to 150 MPa depending on its molecular weight, crystallinity, and orientation of the crystals. Too high crystallinity however decreases significantly its resorbability, leading to compromises between resorption time and mechanical properties. Additionally, PLA can be produced via stereoselective routes, yielding pure PLLA, PDLA, or P(L,D)LA containing predetermined ratios of its two enantiomeric forms. [22]

Polyglycolic Acid (PGA) is another commonly used resorbable polymer in bone fixation and its market is estimated to top $9 billion by 2024. It has been extensively employed and its main characteristics are a relatively fast degradation rate and very high modulus (.ca 6 GPa [23]). Such high crystallinity causes PGA to be relatively brittle, but unlike PLA, doesn't significantly limit its degradability. In fact, the very fast degradation rate is a major complication for massive components, as it can lead to a significant local acidification, in turn causing inflammation and tissue damage. To account for these limitations, it is rarely used pure and often blended with other polymers such as PLA. [24]

In contrast to resorbable materials, the most discussed bioinert polymer in the biomedical sector is most likely Polyether ether ketone (PEEK). It is an engineering thermoplastic that has gained significant attention due to its valuable combination of mechanical properties and biocompatibility, making it a promising material for implants. PEEK shows high tensile strength and elastic modulus, respectively around 100 MPa and 3-4 GPa.These high values are paired with remarkable fatigue, abrasion, and degradation resistance. It is therefore suitable for producing removable (e.g. screws, pins, plates) as well as permanent (cartilage replacement) devices. [25]

2.2.2 Common biomedical fillers

Hydroxyapatite (HA) is a calcium phosphate ceramic material that closely resembles the mineral component of human bones. It is widely used in tissue engineering due to its bioactivity and osteoconductive properties. It is also widely used as a reinforcing agent in polymer matrix composites (PMCs) for its biocompatibility and possibility to tailor its microstructure and composition (e.g. whiskers, porous spheres, trabecular structures, aggregates, calcined, or ion doped). Resorption of HA is a complex process that happens at a very slow rate and is heavily influenced by the sintering temperature and effective specific surface area (SSA). Unsintered, uncalcined HA microparticles are generally considered bioresorbable though it can require 5 or more years. Sintered HA particles with lower SSA, on the other hand, don’t resorb at an appreciable rate, but rather get incorporated (i.e. osteointegrated) in the new tissue effectively forming a biocomposite. Thanks to the similarity of HA to mineral components of bone, its presence is analogous to the naturally occurring apatitic phase and is not thought to cause any issues for the patient. [26–28]

β-Tricalcium phosphate is another commonly used bioactive ceramic filler. It has a similar chemical composition to HA, also being a calcium phosphate phase. β-TCP generally shows lower mechanical properties than HA but a significantly faster resorption rate which can be tuned by changing its crystallinity profile.[29]

Bioactive glasses, such as the 45S5 composition, named “Bioglass”® and supposedly the first of many bioactive ceramics, are glasses based on $Na_2O–CaO–SiO_2–P_2O_5$ systems and their variations, generally containing about 50 mol% of silica. They generally have lower modulus than HA, but display superior osteoinductive and osteoconductive properties that can be tailored by varying the composition. Furthermore, bioactive ions can be added to the glass to promote desired processes or effects, such as angiogenesis, osteoclasts inhibition, or antibacterial properties. [30]

Among the challenges encountered during the production of composites with these fillers, a common issue involves obtaining inhomogeneous dispersions due to particle aggregation and/or orientation. This can lead to anisotropic properties, which could be undesired, or batch-to-batch variations in mechanical properties.

2.2.3 Commercially available resorbable screws

Table 2.2.3 below presents some of the resorbable polymer-based screws for bone fixation currently available on the market, specifying their composition and minimum diameter. It is worth to note that most products were originally developed either as resorbable plate-and-screws for cranio-maxillofacial surgery ([a]), or as interference screws ([b]) for tendon to bone fixation such as in anterior cruciate ligament surgery. With the exception of LactoSorb®, the resorbable plate-and-screw systems are also commercialised for generic bone fracture fixation. It is also worth noting that to the author's best knowledge, all of the currently available resorbable screws are based on matrices of PLA, PGA, or their combinations and variations.

Table 2.2.3: Composition and minimum diameter of commercially available resorbable plate-and-screw systems [a], and interference screws [b].

Product	Producer	Matrix polymer	Filler material	Ref	Min ∅
OSTEOTRANS-MX[a] SuperFIXSORB-MX[a]	TEIJIN Medical Technologies	SR-PLLA	Unsintered µ-HA	[31]	2.0
FIXSORB-MX[a]		SR-PLLA	-	[32]	2.0
RAPIDSORB[a]	DePuy Synthes	PLLGA 85:15	-	[33–35]	1.5
FreedomScrew[a] CPS system[a] OTPS system[a]	Inion Oy	Copolymers of L-, D- lactate, glycolide and trimethylene carbonate	-	[36–38]	1.5
LactoSorb[a]	Zimmer Biomet	PLLGA 82:18	-	[39]	1.5
Biosteon Screw[b]	Biocomposites	PLLA	HA	[40]	6.0
Bioscrew[b]	Conmed	PLLA	-	[41]	7.0
GENESYS Matryx[b]	Conmed	P(L,D)A 96/4	µ-TCP	[42]	5.0

The mechanical properties of these commercialised materials are not hereby reported, as it has proven challenging to obtain standardised comparable data for all of such formulations. It is worth mentioning, however, that among the resorbable plate-and-screw systems, SuperFIXSORB-MX® appears to possess the highest mechanical properties, with flexural

modulus and flexural strength respectively around 12 GPa and 270 MPa [43]. It also appears to have the lowest resorption process, which necessitates .ca 5 years for complete matrix degradation and up to 6 years for complete HA incorporation [31]. The reason for such a long resorption time and high mechanical properties is not made explicit by the inventors, but most likely lies in the very high crystallinity imparted to PLLA during the manufacturing process.

2.3 AdhFix

Within the field of hard tissue repair, but straying from dental fillings, the research group led by prof. Malkoch has developed an innovative system for bone fracture fixation based on triazine-trione (TATO)-derived monomers, named AdhFix. This method is suitable for fractures requiring open reduction internal fixation (ORIF), and involves the mixing of trifunctional TATO-thiols and TATO-alkenes together with a photoinitiator and hydroxyapatite powder (HA) as a reinforcing phase. This yields a paste-like composite that can be shaped to the surgeons' needs and adapted in a patient-specific manner.This composite paste is then applied in the manner depicted by *Figure 2.3* [3] and *in-situ* cured layer by layer via high energy visible light (HEVL). A detailed description of the AdhFix technique is later presented in sections 3.2.1 and 3.2.3 as it is part of this research project.

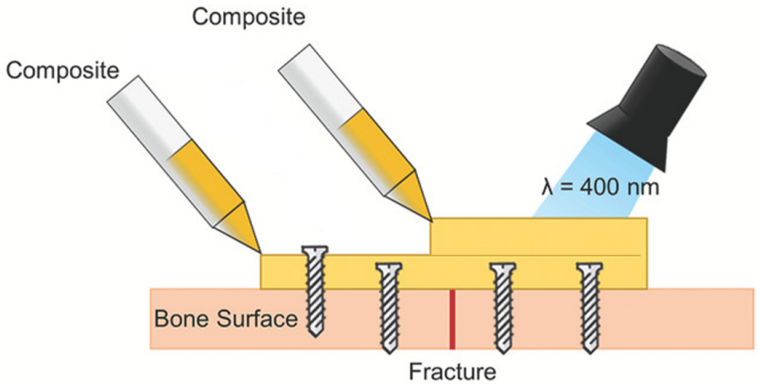

Figure 2.3: Illustration of AdhFix layer-by-layer technique [3]

The ultimate goal of Malkoch's research group is to be able to fix bone fractures adhesively, without the need of using metal screws with a completely bioresorbable system. The challenges in developing such an advanced system are many: even though *Granskog et al.*[44] have developed a significantly improved bone adhesive technology, it is still deemed not reliable enough to be used in clinical applications and it is not bioresorbable. To ensure fixation to the underlying bone, the AdhFix methodology with metal cortical screws was developed. Currently, the main advantages of this technology are the unprecedented possibility for the surgeons to customise the geometry of the patch in situ and the minimal

scar tissue formation due to soft tissue adhesion and damage, improving mobility recovery. However, both due to the presence of metal screws and the inert nature of the composite, it is not bioresorbable[3]. Furthermore, the interface between the metal screws and the composite patch is a critical point, where in some preliminary tests the composite detaches from the screw, leading to failure of the system.

2.3.1 Thiol-ene chemistry

Thiol-ene (TE) chemistry refers to a class of powerful, versatile reactions that has been known since the very beginning of the 20th century, as reported in a widely cited article by *Theodor Posner*[45]. Due to its wide applicability, high efficiency, and mild reaction conditions it has recently been gaining increasing attention. As suggested by the name, these reactions involve the reaction between alkenes and thiol-containing molecules and are broadly divided in two categories according to the reaction route: nucleophile (most commonly a base) promoted in “thia-Michael addition” reactions, while radical initiated for “classical” thiol-ene reactions.

This distinction arises from the nearly opposite reactivity of different alkenes towards thiols when undergoing anionic rather than radical reactions.

The “classic” thiol-ene reactions make use of a suitable radical initiator, generally photo- or thermo- activated (e.g. AIBN, benzophenone derivatives, etc) and follow a peculiar “double loop” mechanism as illustrated in *Figure 2.3.1* [46]. The initiating radical reacts by abstracting a hydrogen from the thiol group, forming a reactive thiyl radical which propagates via anti-Markovnikov radical addition to the alkene’s unsaturated bond to form a thioether alkyl radical. After this step, there are two possibilities:

- Homopolymerization: The alkyl radical keeps propagating by reacting with other alkenes, in a manner analogous to chain-growth polymerization.
- Chain transfer: The alkyl radical abstracts a hydrogen from an available thiol, effectively completing one loop cycle and forming a thiyl radical that is free to react with the next alkene. This pathway leads to a step-growth-like polymerization.

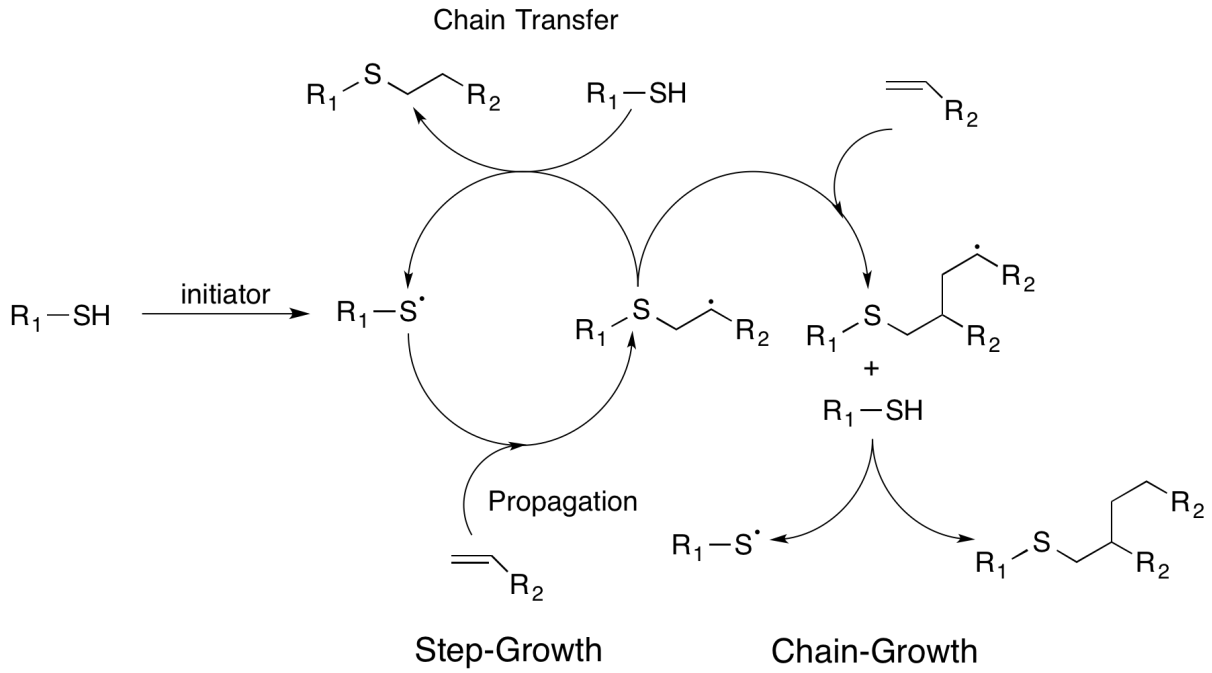

Figure 2.3.1: reaction mechanism of thiol-ene[46]

Such reactions are therefore subject to a combination of step-growth and chain-growth pathways. The relative contribution will be dictated by the reactants availability and chemical kinetics. It has by now been established that it is the nature of the alkene that determines whether the reaction will proceed via step-growth thiol-ene reaction or chain-growth homopolymerization[47]. As an example, methacrylates, widely used in dental restorations, show an enhanced tendency to follow the homopolymerization pathway and a reduced tendency to chain transfer in awe of the greater stability of the radicals they form[48]. Non-homopolymerizable alkenes that form less stable radicals, on the other hand, will mostly follow the step-growth pathway. Thanks to the reactions' advance through hydrogen abstraction steps, oxygen inhibition is very limited, as the formation of a peroxy-radical due to the reaction of oxygen with a alkyl radical is itself reactive enough to participate in the chain transfer by abstracting a hydrogen from an available thiol[49]. The step-growth pathway also ensures a high conversion of the monomers as gelation is delayed with respect to chain-growth mechanisms exploited by methacrylates. Total conversion is desirable not only because of the mechanical properties, but mostly due to the migration and leakage of unreacted monomers which could cause severe adverse reactions at a local or systemic level. A great amount of research has focused on implementing thiol-ene systems in the biomedical field, specifically in dental repair, as TEC systems also show lower curing induced shrinkage stress than methacrylates, therefore reducing the risk of microcracking and detachment from the enamel. A further cause of concern in most dental methacrylates is their content of monomers with structure similar to bisphenol-A, although currently no

adverse effects have been reported [50] Methacrylates however, possess superior mechanical properties, especially in regards to flexural strength and modulus[51].

To enhance the mechanical properties of thiol-ene systems, a large variety of TE monomers based on the TATO ring have been proposed by various research groups[51–53]. The rationale behind such a choice is that small multifunctional molecules would be able to form a highly crosslinked network which is further reinforced by the stiff triazine-trione ring structure. In addition to this, inorganic particles can be added to enhance the stiffness of the material, as in the case of AdhFix previously mentioned.

2.4 Polymer matrix composites

Polymer matrix composites (PMCs) have seen an incredible expansion starting in the 1960's and 70's because of the possibility to achieve light and strong materials. Even nowadays, the demand for PMCs is dominated by automotive, aeronautics and construction industries[54]. The possibility of combining properties from different classes of materials led to an explosion of opportunities in all sectors, including the biomedical sector, where implant materials could be made tougher, stronger, or given an array of desirable functionalities, such as being more biocompatible, anti-inflammatory, or even able to promote tissue regeneration[55]. The current AdhFix method falls within the category of particulate reinforced PMCs (PRPMCs), where HA is the reinforcing filler.

The need for a deeper understanding of the interaction between matrices and fillers has led to the development of different theories of reinforcement. Such theories are not mutually exclusive, but rather generally describe one of the mechanisms that contribute to the final mechanical properties of the composite. In order to have a complete view of the system, theories often have to be combined to take into consideration all the influencing factors. In other cases, one of the proposed reinforcing mechanisms is predominant and for the sake of simplicity, the other ones can be considered irrelevant without committing substantial mistakes[56]. Notably, most theoretical models regarding particle-reinforced composites were developed to estimate the elastic modulus of a composite, and can be divided into two categories based on the starting assumption[57]:

Rigid inclusions in a non-rigid matrix base their derivation on the viscosity theories for solid-liquid suspensions, as is the case of *Einstein*, *Mooney*[58], or *Kerner's*[59] models.

Rigid inclusions in a rigid matrix: lead to the elementary series and parallel models (respectively *Reuss'* and *Voigt's* models)[55]. More advanced models employ a combination of these such Takayanagi's [60] model. Others consider the influence of the aspect ratio

such as Chow[61], while Cox [62]assumes that for high aspect ratio inclusions, stresses are transferred only through shear mechanisms.

On the other hand, far fewer theoretical models were developed to estimate the yield strength of particle-reinforced polymers. The vast majority of estimation methods are in fact semi- if not entirely empirical, being applicable only in satisfactorily characterised systems. Most models however agree that surface-related (area, adhesion, geometry) parameters play a key role in determining the final composite's strength, and are sufficiently explained by the following particulate reinforcement theories.

Interfacial adhesion theory: As a composite material experiences a load, this will be transferred from the matrix to the filler via their interface. It is therefore logical that in order to have an efficient transfer of stress, it is crucial that there is good adhesion between the polymer matrix and the reinforcing particles' surface. This implies also that fillers with a higher specific surface area will be more efficient reinforcing agents, as a larger interface will be available for stress transfer. Therefore, particles having a lower size or a higher aspect ratio will be more effective[63].

Crystallization-inducing theory: It has been found that inorganic fillers influence the polymer's crystallization process when cooling down a PMC melt [64,65]. Inorganic particles act as heterogeneous nucleation points, therefore accelerating the crystallization of the polymer and ensuring improved mechanical properties in awe of a higher crystallinity. This effect however is somewhat inhibited at higher filler loadings as the filler particles can reduce the polymer's chain mobility.

For PMCs that are highly crosslinked and solidify rapidly, the latter mechanism plays a minimal role, as very limited crystallization is possible. For this reason, in applications where higher performances are required, filler particles often undergo compatibilization treatments, as in the case of silanization for silica fillers in dental composites[51].

Notably, many models for elastic modulus estimates of PRPMC do not include a parameter accounting for interfacial adhesion, as empirical data also suggests that the elastic modulus is not significantly affected by it, with filler loading and geometry being the main influencing factors [63]. The most effective models for estimating yield strength on the other hand generally do include a term for interfacial adhesion as it majorly affects the output value.

The generally accepted theories for adhesion can be used to understand particle-matrix compatibility and are therefore hereby summarised.

- **Physical adsorption/wetting** theory sets the essential prerequisite for good adhesion with any substrate. The adhesive phase (i.e. polymer matrix) should come in contact with the particles' surface and wet it in order to establish an adhesive bond. Wettability is regulated by relative surface energy, which is itself dependent on the chemical nature and microstructure of the surfaces. When the particles are wetted by the matrix, primary (covalent) or secondary (van der Waals, H-bonding) interactions will contribute to the adhesive bond depending on the available chemistries [66]. It is important to note that secondary interactions are much more sensitive towards their environment than covalent ones. For instance, H-bonds can be disrupted by the small water molecules present in many environments[67].

- **Mechanical interlocking** occurs when the adhesive phase is able to flow into pores, cavities or other irregularities on the substrate's surface. Once solidified, the matrix and fillers are mechanically locked together, significantly increasing the stress transfer efficiency. This is a major mechanism when dealing with porous structures.

- **Diffusive theory** is similar to mechanic, but the migration of the adhesive occurs on a molecular level, where molecules of adhesive and substrate interdiffuse to create an interphase region exhibiting a gradual variation of properties with no clear interface. This mechanism requires inter-solubility of the molecules, and is therefore relevant only in such cases, not for inorganic particles in PMCs.

- **Electrostatic theory** addresses the electrostatic forces which develop at the substrate-adhesive interface, mainly caused by the formation of an electric double layer or difference in electronic band structures. These forces are often very small with respect to other interactions and are often neglected or considered minimal if not in specific cases [66].

2.4.1 Surface compatibilization

When considering inorganic PRPMCs, the two most useful explanations originate from the adsorption and mechanical interlocking approaches. A great amount of attention is in fact placed upon investigating the best compatibilizing systems for a range of biomedical fillers, such as silica glass [68,69], bioactive glass [70] HA [71,72], alumina [73], titania [74], and more. Two main classes of compounds are used to compatibilize oxide surfaces: alkoxysilanes and phosphonic acids. Compatibilization is achieved in a somewhat similar fashion to surfactants: the phosphonic or silanol groups condense with the hydroxyl groups present on the oxidic surface to create one or more covalent bonds, as illustrated in *Figure 2.4.1* [75]. To optimise the polymer matrix-R group interaction, the latter can be tailored to be

more or less hydrophilic, longer, shorter, or contain other functional groups that can in turn covalently bond to the polymeric matrix.

Relatively recently, differences in performances of these two classes have been studied towards different substrates and can be briefly summarized as follows. Alkoxysilanes show greater hydrolysis resistance when applied on silica-based oxides; on the other hand, phosphonic acids form a more stable P-O-M bond, when the metal M is not silicon. In other words, phosphonate compatibilizers appear to be more durable than their silanol counterparts when applied on non-silica oxides such as alumina [75,76].

Alkoxysilanes are also prone to nucleophilic substitutions, which makes them easily hydrolyzable and predisposed for homocondensation other than heterocondensation with the oxidic substrate. Phosphonate derivatives on the other hand, are substantially less sensitive to nucleophilic substitution, and heterocondensation with oxidic surfaces is thermodynamically favoured, while homocondensation only occurs under dehydrating conditions at high temperatures. This leads to phosphonic acids generally forming a single "bidimensional" monolayer, while alkoxysilanes can form three-dimensional multilayers as respectively illustrated in *Figure 2.4.1 (L)*and *(R).* [77]

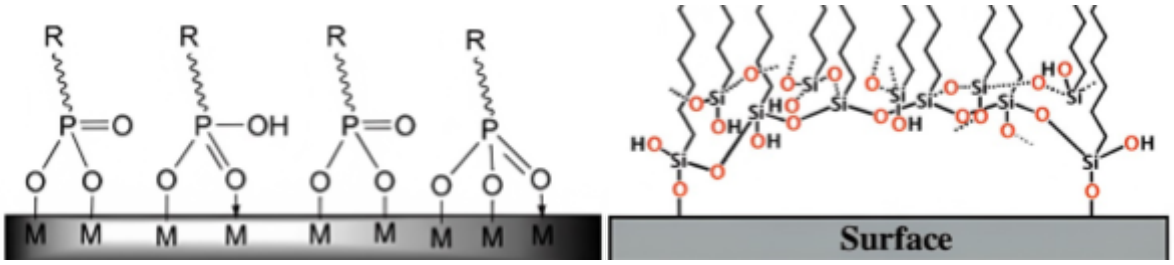

Figure 2.4.1: Schematic representation of phosphonate surface compatibilizers (L) [75] as well as a proposed schematization of organosilanes surface compatibilizers (R) [77].

2.4.2 Composite production technologies

Virtually all fibre-reinforced composite materials are fabricated in laminates and assembled layer by layer, however, PRPMCs are generally fabricated by casting methods or injection moulding. To these, degassing stages are added when the requisites of the product are such that presence of air bubbles is undesirable. It is the case of most PMCs that must withstand significant loads, where a density as close as possible to the theoretical is desired. More complex processes can be employed when specific effects want to be achieved. For example, *Shikinami and Okuno* report compounding PLLA and HA particles with an extruder to obtain a thick billet which undergoes a forging process, whose compression forces rearrange the crystal orientation. To maintain the as-forged microstructure, the material is

then cut and machined to the desired geometry [43]. More generally, existing literature indicates processes such as injection-, compression-, and injection transfer- moulding as suitable production techniques for resorbable screws. More detailed information (e.g. exact molecular structure, processes parameters, etc) is however kept highly confidential from the producing companies.[78]

3. Experimental

3.1 Instrumentation, chemicals and materials

3.1.1 Chemicals and materials:

All chemicals were purchased from commercial vendors and used as received. Magnesium sulphate (97%, anhydrous) (MgSO4) was purchased from Acros Organics. Irgacure 819 was purchased from Ciba Specialty Chemicals Inc. $CDCl_3$, DMSO-D_6, DCM, 10-undecenoic acid and EtOAc, were purchased from Fisher Scientific. HA whiskers and MCD apatitic abrasive powder were purchased from Himed. Bioglass (58S, 10 ≤ μm), HA, TATATO, γ-MPS, 3,6-dioxa-1,8-octane-dithiol (95%), 4-pentenoic acid, diethyl (hydroxymethyl)phosphonate, 5,5'-dithiobis(2-nitrobenzoic acid) (DTNB), were purchased from Sigma Aldrich®. PET mesh was obtained from Surgical Mesh™. CDI was purchased from Tokyo Chemical Industry Co., Ltd. SYLGARD® 184 silicone elastomer kit was purchased from Dow Inc. Acetone, ethanol, methanol, isopropanol and acetic acid (99-100%) were obtained from VWR. Proprietary catalyst (catalyst) was obtained from the Division of Coating Technology at KTH.

3.1.2 FT-Raman spectroscopy

FT-Raman analyses were performed on a Jovin Yvon Raman Confocal Microscope (HR800 UV) instrument using a green 532 nm laser source. The scans were performed from 0 cm^{-1} to 4000 cm^{-1} with an exposure time of 3 s and 8 repetitions.

3.1.3 1H-NMR and 13C-NMR

NMR measurements were performed on a Bruker Avance AM 400 instrument at 298 K with 128 scans for 1H-NMR and 256 scans for 13C-NMR. $CDCl_3$ or DMSO-D_6 was used to dissolve the samples with a concentration of 30 mg/mL. The spectra were referenced to the internal solvent signal. All chemical shifts are reported in δ (ppm). All NMR spectra are presented in appendix I.

3.1.4 SEM

SEM analysis was performed using a Hitachi TM-1000 SEM machine with a voltage of 15kV in standard emission mode. Powders were observed without further treatments by dispersing them on conductive carbon tape. Using a Cressington 208HR sputter coater with Pd target, fracture surfaces were first coated with 3-5 nm of Pd and successively observed with the SEM.

3.1.5 UV-Vis

UV-Vis spectrophotometry was performed with a Shimadzu UV-2550 UV-Vis Spectrophotometer. Absorbance was measured at 412 nm for cysteine standards and thiol-functionalized fillers' supernatant treated with Ellman's reagent (DTNB).

3.1.6 FT-IR spectroscopy

Fourier-transform infrared spectroscopy (FT-IR) was performed on Spectrum 100 FT-IR instrument equipped with a single reflection ATR system and a MIR-TGS detector using an MKII Golden Gate and a diamond crystal (Graseby Specac Ltd, Kent, England). Wavelength range: 600-4000 cm^{-1}, 16 scans averaged at 4.0 cm^{-1}.

3.2 Methods and procedures

3.2.1 Composite formulation:

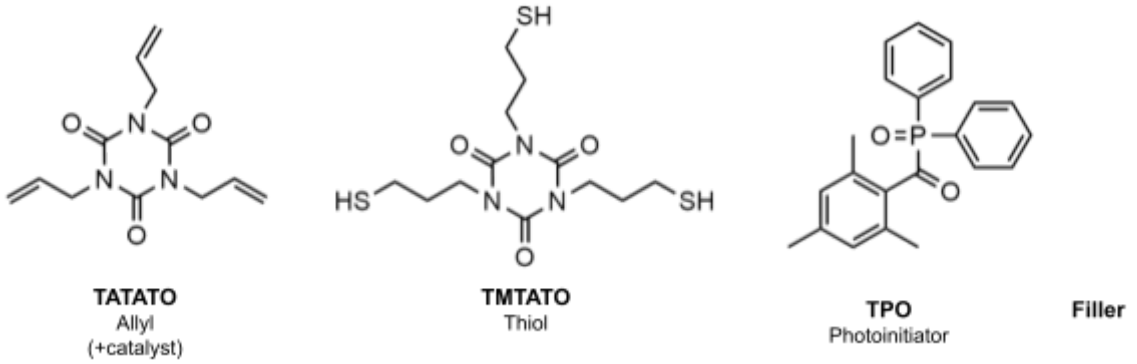

The prototype formulation for the AdhFix composite contains the above ingredients and is processed as follows. A solution of TATATO (12.4 g) and catalyst (0.7 g) (TATATO+cat) is pre-made and can be stored at room temperature. TMTATO (1810 mg) and the premade solution of TATATO+cat (1310 mg) are mixed in a glass vial with a closed-off glass pipette. The vial is then wrapped in aluminium foil and the photoinitiator, TPO (17.8 mg), is

incorporated by stirring with the closed-off glass pipette for about 1 min. Finally, the filler is stirred in according to the desired weight percentage. The composite is allowed to rest for a minimum of 15 min, shielded from light with aluminium foil.

In this report, the composite containing 56wt% of HA as filler is referred to as ***prototype formulation***, being the current standard used in the AdhFix technique.

3.2.2 Composite degassing:

Some of the formulations underwent a degassing process prior to curing to ensure a reduced porosity. Degassing was performed immediately after the filler addition by closing the vial with a rubber septum and attaching it to a Schlenk line's vacuum through a needle for 1.5 h. When degassing the composite for bone fixation patches (BFPs), vacuum was applied for 1 hr instead. Aluminium foil was wrapped around this setup to ensure complete shielding from external light.

3.2.3 Curing of TE Composite Formulation:

Curing was achieved as described by Granskog et al.[44]. The adhesives were cured using a light-emitting diode (LED) polymerization lamp (Bluephase 20, Ivoclar Vivadent AG, Liechtenstein), wavelength (λ) of 385–515 nm with λ_{peak} at 400 and 470 nm and a maximum

intensity of 2000 mW cm−2, intended for light-cured dental materials for 10 s per surface area. The reduced intensity or absence of alkene (C=C) and thiol (S-H) peaks in FT-Raman spectrum indicated satisfactory curing of the resin. FT-Raman of the resin: [ν(S-H) 2575 cm^{-1}], [ν(C=C) 1646 cm^{-1}].

3.2.4 Porosity determination with Fiji-ImageJ

Fracture surface of prototype formulation beams were observed with the tabletop SEM. Micrographs were taken at 120x magnification for three beams. Brightness and contrast of the images was adjusted according to the operator's judgement to better distinguish the pores from pull-out marks. The pores were manually filled with black ellipses and the other components were eliminated by adjusting the passing threshold. Via the *analyse particles* feature of the Fiji-ImageJ software [79], the area fraction of each pore was obtained and exported on a spreadsheet, where it was summed to obtain an estimate of total porosity. The results from three beams were then averaged.

3.2.5 Mechanical testing of TE composite formulations:

Beams of the TEC composite materials were manufactured in PTFE moulds sandwiched between glass slides at both apertures, with approximate dimensions of 40 × 6 × 1.6 mm (l × w × t), and photocured as previously described. Mechanical performance was evaluated by three-point bending in an Instron 5566 universal testing machine (Instron Korea LLC) using a 500 N load cell with a cross-head speed of 1 $mm \cdot min^{-1}$, a preload of 0.1 N, and a preload speed of 0.5 $mm \cdot min^{-1}$. The centre-to-centre distance of the lower contacts was 30 mm. All measurements were conducted at 20 °C with a relative humidity of 50%. The data were collected using Bluehill software. Mechanical properties were calculated via elastic beam theory equations. Three to five specimens were tested for each formulation.

3.2.6 Silicone mould production:

SYLGARD™ 184 two component silicone was used to fabricate screw moulds. The silicone monomers and curing agent were mixed in a 10:1 ratio by mass and placed 1 h at 4 °C to allow for air removal. The model screw was placed perpendicularly in a 5 mL cylindrical glass vial and covered with the silicone mixture. The vial was allowed to rest for 1 h at 4 °C, then any leftover air bubbles were removed with a vacuum system. The vial was finally placed at 70 °C overnight for curing, after which the vial was broken and the screw removed to obtain a cured, transparent silicone mould.

3.2.7 Composite screws production:

After degassing, the composite was transferred in a 10 mL plastic syringe covered in aluminium foil, placed in a vertical position and degassed again for 15 minutes in a vacuum desiccator. The composite was then injected in the silicone mould in a fashion analogous to bottom pouring in steelmaking: the needle was used to pierce through the silicon from the lower side and the composite was injected until it just started to overflow from the top. The syringe was then removed and a small cross-head screwdriver was used to impress the drive's shape before curing. The composite was cured by shining HEVL through the silicone mould, then extracting the screw and curing again with a method analogous to that previously described albeit modified for the current geometry. Some screws required sanding of the head to ensure a more regular shape.

3.2.8 Cytotoxicity - preliminary study

Human keratinocytes (HaCaT) were used for the cytotoxicity assays. The cell line was obtained from ATCC and maintained in tissue culture flasks at 37 °C in CO_2 (5%) with

Dulbecco's modified Eagle's medium (DMEM), supplemented with foetal bovine serum 10% (v/v), l-glutamine (4 mM), penicillin (100 IU/mL), and streptomycin (100 µg/mL). Cells were harvested and transferred into 96-well plates at a concentration of $1 \cdot 10^4$ cells per well in 100 µL DMEM cultured 24 h before use. To test the cytotoxicity of the fillers, the particles were dispersed in media at the desired concentrations (0.5, 1 mg/mL), then 100 µL added to the 96-well plates and incubated with cells for 48 h. Subsequently, Alamar Blue (resazurin) (10 µL) was added, and incubation was continued for 4 h. The plate was then shaken for 20 s and the fluorescence intensity was measured with a plate reader (Tecan Infinite M200 Pro) at excitation/emission wavelength of 560/590 nm. All results are shown as arithmetic mean ± SD.

The cytotoxicity of the composites was assessed using a human keratinocyte (HaCaT) cell line. The cells were harvested and seeded in 96-well plates at a concentration of $1 \cdot 10^4$ cells per well in 100 µL DMEM and cultured 24 h before use. The composite was formed with a total surface area of 3 cm^2 and sterilised under UV light for 20 min. After sterilisation, the composite was immersed in 1 mL of cell culture medium (3 cm^2/mL) and transferred into the incubator for 24 h at 37 °C. 100 µL of the composite elute solution was then added to the 96-well plates and incubated with cells for 48 h. After incubation, Alamar Blue (resazurin) (10 µL) was added, and incubation was continued for 4 h (37 °C, CO_2 (5%)). The plate was then shaken for 20 s and the fluorescence intensity was measured with a plate reader (Tecan Infinite M200 Pro) at excitation/emission wavelength of 560/590 nm. All results are shown as arithmetic mean ± SD.

3.2.9 AdhFix application on model transverse fractures:

Porcine 2nd and 5th metacarpals have been used as bone substrates as they possess similar shape to human phalanxes [80]. These were dissected from porcine feet from a local butcher, then cleaned from soft tissue, wrapped in wet tissue and stored in a freezer until needed. For usage, the bones were allowed to defrost at room temperature, then cut in half with a hand saw to model a transverse fracture. Four holes were then drilled with a 1 mm drill bit, two on each bone piece and spaced 5-7 mm apart, into which metal screws (1.5 or 2.5 mm nominal diameter) were inserted to about 80% of their length. The composite was then applied around the screw shanks with a closed-off glass pipette, then screws were tightened and the composite cured with HEV light from a dental lamp as described in the curing section. The fracture was reduced by aligning the bone pieces with light pressure, then a thin layer of composite was applied across the fracture to bridge the composite across it and cured. Further layers of composite were applied and cured to reach the desired geometry. The patched bone was then wrapped with wet tissue until mechanical testing.

3.2.10 Evaluation of AdFix on porcine metacarpals

Evaluation of AdhFix fixations' strength on porcine metacarpals was performed as previously reported in the Malkoch group by *Hutchinson et al.* [3]. Briefly, three-point bending was employed in an Instron 5566 universal testing machine (Instron Korea LLC) equipped with a 10 kN load cell. All measurements were taken with a relative humidity of 50% and a temperature of 20 °C. The centre-to-centre spacing between the lower contacts was set at 35 mm. The load and displacement were measured with a cross-head speed of 5 mm/min, a preload of 1 N, and a preload speed of 2.5 mm/min. The fixations' bending rigidity was calculated in the initial elastic region of the load (F) vs displacement (Y) curve using *Equation (1)* , where L is the distance between the lower contacts [81].

$$Bending\ rigidity = \frac{L^3 \Delta F}{48 \Delta Y} \qquad \textbf{Equation (1)}$$

3.3 Synthesis of monomers

3.3.1 Synthesis of TTSAc from TATATO

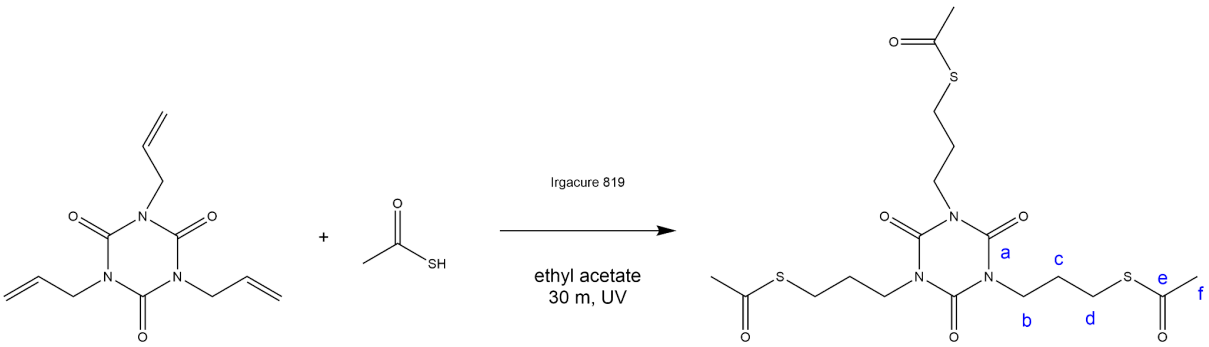

TATATO **Thioacetic acid** **TTSAc**

Thioacetic acid (49.96 g, 0.6565 mol), TATATO (49.97g, 0.2004 mol) and Igracure 819 (0.50 g, 0.0012 mol) were dissolved in ethyl acetate (88 mL) with stirring at room temperature. The yellow solution was then exposed to UV light (λ_{max} = 365 nm) continuously while stirring for 30 minutes. The reaction resulted in the evolution of a small amount of heat, and a change in colour of the solution from dark yellow to light yellow. The absence of TATATO's alkene peaks in the ^{1}H NMR spectrum indicated that the reaction was complete. The solution was diluted with ethyl acetate (200 mL) and washed with $NaHCO_3$ 10% solution (4 x 50 mL) and brine (3 x 50 mL). It was then dried over $MgSO_4$ and rotary evaporated to give a light yellow oil. The product was then recrystallized from MeOH (400 mL) to give **TTSAc** as white

crystals (84.9 g, 88.7%). ^{1}H NMR ($CDCl_3$, 400 MHz), δ/ppm: 3.95 (6H, t, *J*=7 Hz, H2), 2.88 (6H, t, *J*=7 Hz, H4), 2.31 (H9, s, H6), 1.93 (6H, p, *J*=7 Hz, H3). ^{13}C NMR ($CDCl_3$, 101 MHz), δ/ppm: 195.5 (C5), 149.1 (C1), 42.1 (C2), 30.7 (C6), 28.1 (C4), 26.3 (C3).

3.3.2 Synthesis of TMTATO from TTSAc

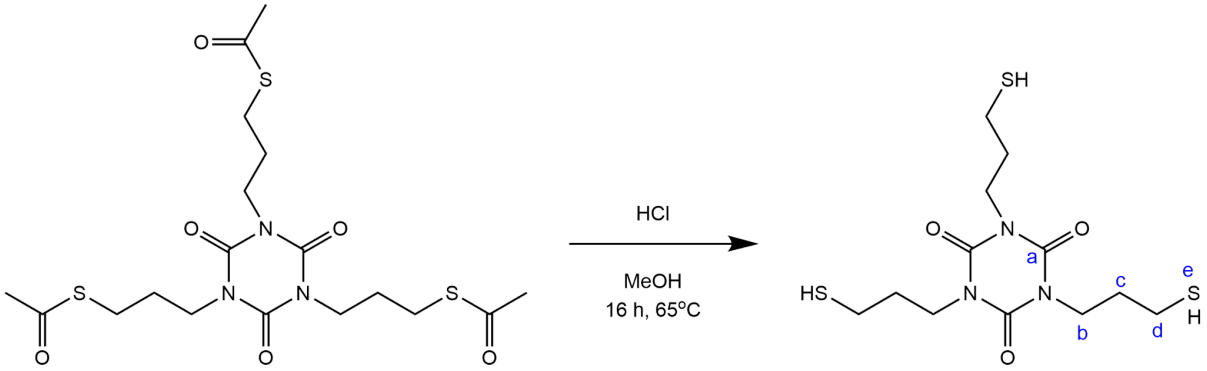

TTSAc **TMTATO**

Synthesis is adapted from literature procedure[53]. A solution of **TTSAc** (43.73g, 0.0916 mol), HCl (100 mL) and MeOH (180 mL) was stirred at 65°C overnight. The reaction was purged with distilled water (250 mL) and then extracted with EtOAc/heptane 50:50 (1 x 450 mL + 3 x 150 mL). The extracts were washed with brine (1 x 130 mL), $NaHCO_3$ 10% solution (3 x 130 mL), water (3 x 130 mL), and brine (1 x 130 mL), dried over $MgSO_4$, evaporated and dried *in vacuo* over 48 h to give **TMTATO** as a clear, colourless oil (31.0 g, 96%). ^{1}H NMR ($CDCl_3$, 400 MHz), δ/ppm: 4.01 (6H, t, *J*=7 Hz, H2), 2.56 (6H, dt, *J*=7, 8 Hz, H4), 1.96 (6H, p, *J*=7 Hz, H3), 1.53 (3H, t, *J*=8 Hz, H5). ^{13}C NMR ($CDCl_3$, 101 MHz), δ/ppm: 149.1 (C1), 42.0 (C2), 32.0 (C3), 22.1 (C4).

3.3.3 Synthesis of C-5 Phosphonate-Protected (PEMPA-Et)

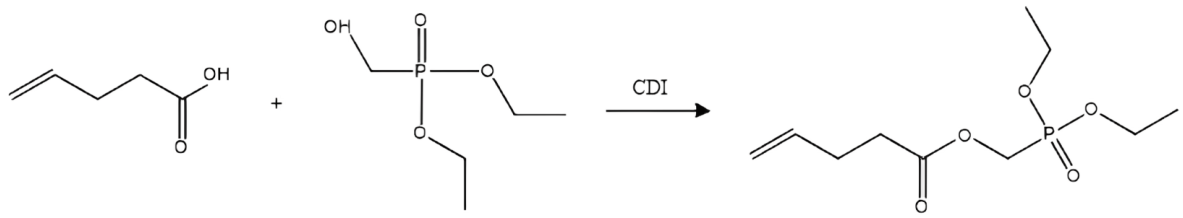

4-Pentenoic acid (3 g) was added in a round bottom flask and diluted with EtOAc (60 mL). CDI (5.83 g) was then added portion-wise and left stirring at room temperature for 2 h.

Diethyl (hydroxymethyl)phosphonate (5.04 g) was added and left to react 24 h. The reaction was quenched with water (75 mL) and washed with $NaHCO_3$ 5% solution (1 x 20 mL), $NaHSO_4$ 5% solution (3 x 20 mL), and brine (1 x 20 mL), dried over $MgSO_4$, evaporated and dried *in vacuo* over 24 h to give (diethoxyphosphoryl)methyl pent-4-enoate as a clear light-yellow oil (4.43 g, 59%). The product was then purified via silica column using EtOAc as the eluent (3.35 g, 76%).

3.3.4 Synthesis of C-11 Phosphonate-Protected (UEMPA-Et)

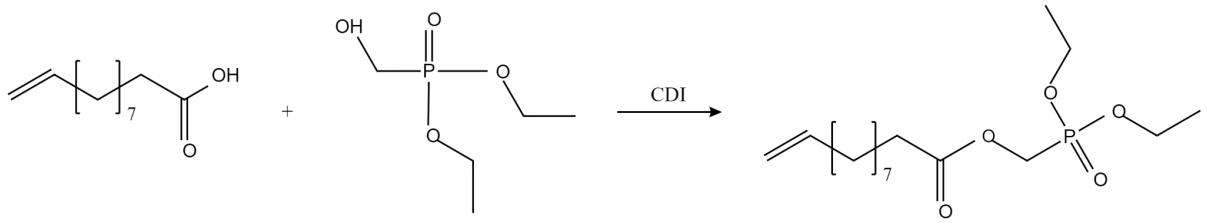

10-Undecenoic acid (10 g) was added in a round bottom flask and diluted with 100 mL EtOAc. CDI (10.58 g) was then added portion-wise and left stirring at room temperature for 2 hours. Diethyl (hydroxymethyl)phosphonate (9.13 g) was added and left to react for 24 h. The reaction was quenched with water (40 mL) and washed with $NaHCO_3$ 5% solution (1 x 35 mL), $NaHSO_4$ 5% solution (3 x 35 mL), and brine (1 x 35 mL), dried over $MgSO_4$, evaporated, and dried *in vacuo* over 48 h to give (diethoxyphosphoryl)methyl undec-10-enoate (UEMPA-Et) as a clear light-yellow oil (16.54 g, 91%).

3.3.5 Synthesis of C-5 Phosphonic acid (PEMPA)

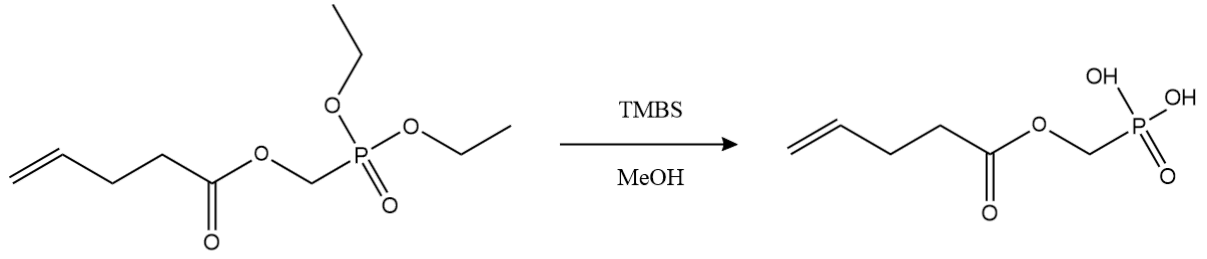

(diethoxyphosphoryl)methyl pent-4-enoate ((pent-4-enoyloxy)methyl)phosphonic acid

TMBS (3.2 g, 0.0209 mol) was slowly added to a solution of PEMPA-Et (3.2g, 0.0128 mol) in $CHCl_3$ (12 mL), stirring at 0°C. The mixture was stirred at room temperature overnight, then evaporated to dryness. The resulting brown oil was dissolved in MeOH (27 mL) and stirred at room temperature for 2 h. The MeOH was then removed by rotary evaporation, and the dark brown solid was dissolved in DCM (20 mL) and evaporated twice. The solid was then dried in vacuo to give PEMPA as a light brown solid.

3.3.6 Synthesis of C-11 Phosphonic acid (UEMPA)

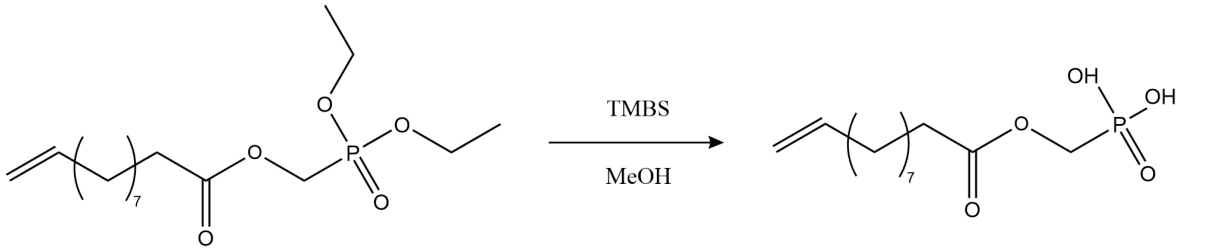

(diethoxyphosphoryl)methyl undec-10-enoate ((undec-10-enoyloxy)methyl)phosphonic acid

TMBS (10.41 g, 0.068 mol) was slowly added to a solution of UEMPA-Et (11.37 g, 0.034 mol) in $CHCl_3$ (33 mL) stirring at 0°C. The mixture was stirred at room temperature overnight, then evaporated to dryness. This resulting brown oil was dissolved in MeOH (44 mL) and stirred at room temperature for 2 h yielding a dark red-brown solution. The MeOH was then removed by rotary evaporation and the brown solid was dissolved in DCM (33 mL) and evaporated twice. The solid was then dried in vacuo to give ((undec-10-enoyloxy)methyl) phosphonic acid (UEMPA) as a brown sticky solid (4.61 g, 75%).

3.3.7 Functionalization of HA-w

The functionalization of HA-w with phosphonic acids was performed as follows: HA-w was dispersed in stirring MeOH (7 mL/g). 3 wt.% of the respective phosphonic acid was then added and left reacting overnight. The particles were then centrifuged, washed with MeOH, and centrifuged again repeating this process 5 times. They were finally dried in a vacuum oven at 80 °C overnight.

3.3.8 Functionalization of BGL

Functionalization of BGL was performed as follows: γ-MPS (0.2 g) was dissolved in 90:10 wt. ethanol:water solution (130 mL). The pH was adjusted to pH 4 with acetic acid. BGL was then added (8.8 g) and left stirring overnight. The particles were then centrifuged, washed with ethanol 96%, and centrifuged again repeating this process 5 times. They were finally dried in a vacuum oven at 80 °C overnight.

3.3.9 Determination of functional groups concentration

1. Thiolation of functionalized particles: 3,6-Dioxa-1,8-octane-dithiol was dissolved in EtOAc (80 mL for every 1 g of particles) . The amount of dithiol was estimated as to be in large excess with respect to the eventual allyl moieties imparted by functionalization on the particles and set to be 1:2 wrt the particles in mass. Irgacure 819 (5wt% wrt dithiol) was then

added together with the particles and stirred for 5 minutes. UV light (λ_{max} = 365 nm) was shined continuously through the solution for 30 min while stirring. The particles were centrifuged, washed with EtOAc, and centrifuged again repeating this process 5 times, then finally washed once with EtOH 96% and centrifuged again. They were finally dried in a vacuum oven at 80 °C overnight, yielding particles with available thiol groups theoretically in a 1:1 ratio to the primary allyl groups.

2. Sample and calibration curve preparation: Ellman's reagent method was adapted from literature [82] to quantify the concentration of thiol groups. Briefly, a 0.1 M potassium phosphate pH 8 buffer solution with 1 mM EDTA was prepared. Ellman's reagent solution (ERS) was prepared by dissolving DTNB in the buffer at 4 mg/mL. To build the calibration curve, cysteine standards of 1,2,4,8,16,32 µM were produced by dissolving cysteine in the buffer solution. ERS (10 µL) was added to 3 mL of each of the standards and placed on a shaking table for 5 minutes. Both thiol-functionalized and control particles (200 mg) were dispersed in the buffer (4 mL), then ERS (13.75 µL) was added and left to incubate on a shaking table for 5 min, after which they underwent centrifugation and the supernatant was collected. Unfunctionalized particles that underwent the same treatment in **1.** were used as control.

3. Absorbance reading: The cysteine standards and the supernatant samples were analysed using a UV-Vis spectrometer measuring the absorbance at λ=412 nm.

4. Results

4.1 Current AdhFix technology

As a starting point, the currently used AdhFix methodology was screened with regards to mechanical properties of the composite and of the fixation system by three-point bending and the fracture surface was observed with a tabletop SEM to analyse its behaviour.

The naming procedure adopted in this thesis for the composites is as follows:

THIOLxALKENE (WT%)FILLER

As an example, the standard composition for AdhFix, as reported in *section 3.2.1*, is hereby presented as TMTATOxTATATO 56HA, where TMTATO is the thiol, TATATO the alkene and HA the filler, in a final concentration of 56 wt%. The photoinitiator (TPO) and the catalyst are present in constant proportion with the monomers, as reported in *section 3.2.1*.

Every new batch of TMTATO used to formulate the standard TMTATOxTATATO 56HA composite and should be mechanically tested to compare it with previous results. If the properties fall within the conventional values, it is good for usage. The results of 3 point bending (3PB) on two beams of the prototype composite were found to be acceptable and are presented in *Table 4.1.a* together with those of the unfilled system. Results for the unfilled system were obtained by D. J. Hutchinson.

Table 4.1.a: Mechanical properties of TMTATOxTATATO systems

Sample	E_f [GPa]	σ_f [MPa]	Flex strain [mm/mm $\cdot 10^{-3}$]	Energy at break [mJ]
Unfilled	2.9 (0.4)	99 (6)	96 (26)	95 (9)
56HA	6.6 (0.1)	59 (1)	9.6 (0.2)	11.4 (0.2)

Following the mechanical testing, the fracture surface of these two samples was observed via a tabletop scanning electron microscope (SEM) with a 3 nm .ca Pt/Pd coating. An image of one of the samples' fracture surfaces is presented in *Figure 4.1* below at lower (a, b x80), and higher (c, x800) magnifications. Via the use of an open-source image analysis software (Fiji-ImageJ[79]), the porosity of the TMTATOxTATATO 56HA composite as produced in sections 3.2.1; 3.2.3 was estimated to be 20±5%. Although smaller pores were observed at higher magnifications, the minimum equivalent diameter for pore detection was set at 5 μm, as smaller ones would have required more effort to differentiate from cavities left from filler pull-out or detachment. The size range was remarkably wide, spanning from 5 to over 450 μm of area-equivalent diameter. Such a high porosity is thought to significantly affect the mechanical properties of the material, simply by reducing the volume of material that can actually sustain an applied load.

Figure 4.1 (c) also shows significant features of the HA particles and of its interactions with the polymer matrix. The HA appear to be secondary particles, that is, aggregates of smaller primary HA, much like unsintered HA [27,83], giving them an intrinsically high interconnected porosity. This implies a very rough surface which could promote mechanical interlocking with the matrix, however, it could also involve poor cohesive strength within the aggregate itself, not granting the desired reinforcement. Besides the presence of significant pores, it is clearly visible how the HA particles are not adhering well to the polymeric matrix, with visible spacing between the matrix and the particles and extensive particle detachment rather than their cohesive failure. While cohesive failure of the fillers is sometimes undesirable, this is mostly the case for fibre reinforced ceramic matrix composites, where fibre pull-out plays a major role in toughening the material. To allow for toughening through fibre pull-out rather

than brittle failure, a carefully balanced interfacial bonding strength is required. Too strong bonding would result in brittle failure of the fibres along the fracture plane, too weak bonding doesn't allow effective stress transfer, lowering the material's mechanics. In the case of particle reinforced composites (PRCs), pull-out is not a significant toughening mechanism as the sphere-like shape doesn't allow for dissipative friction with the matrix. In the case of PRCs such as in AdhFix, it is preferable to maximise the interfacial adhesion to improve modulus and strength of the material. [56]

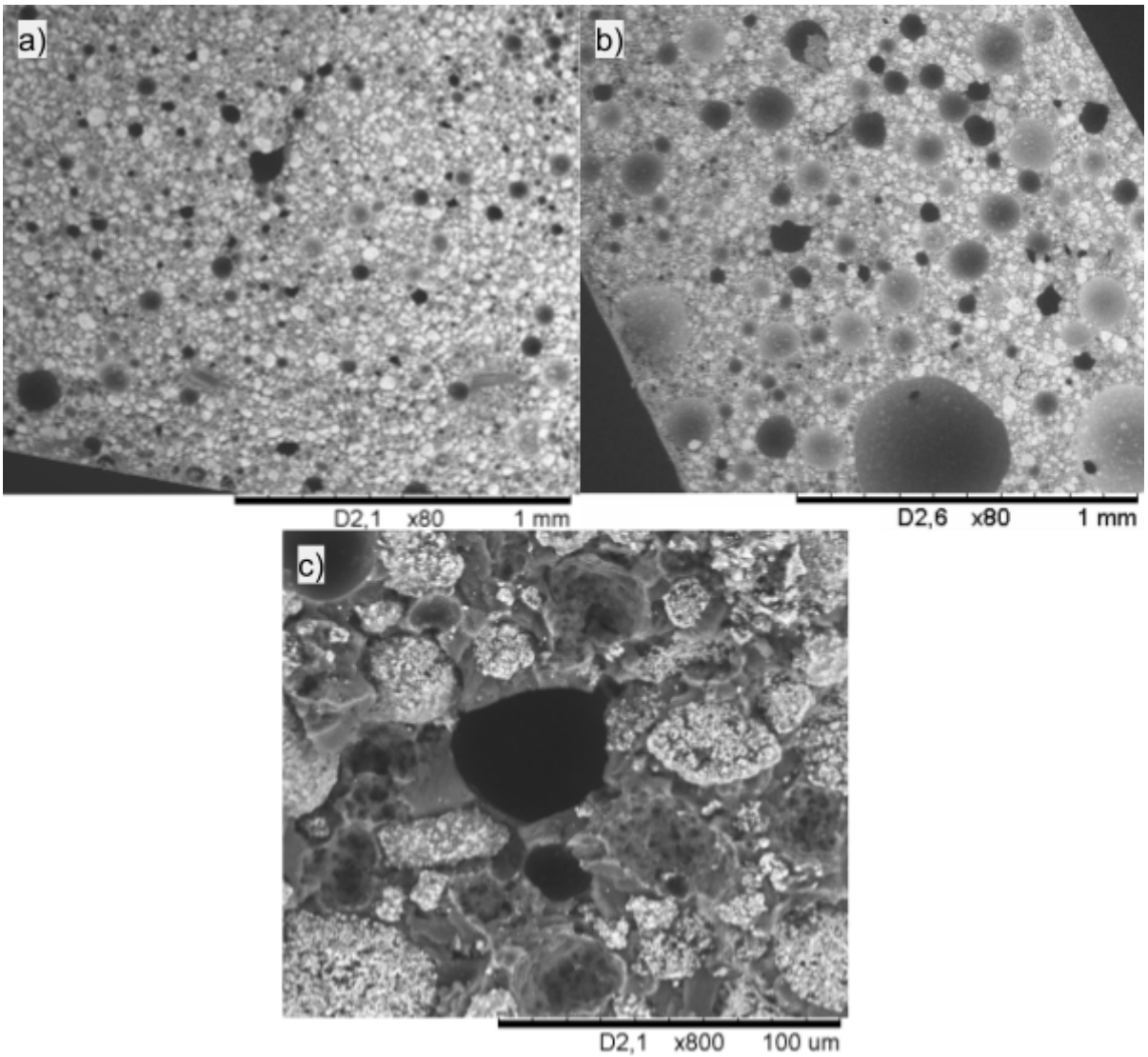

Figure 4.1: TMTATOxTATATO 56HA fracture surface at 80x (a,b) and 800x (c)

The standard composition was used to test screw-making viability and potential criticalities of the process for different screw diameters. Different diameter screws were made from both the 56HA composite and the pure thermoset TMTATOxTATATO as described in section 3.2.7. They were then screwed in and out (if possible) of a porcine metacarpal previously tapped with a steel screw of the same geometry. *Table 4.1.b* below shows how many screws could be successfully inserted (✅) or failed (❌) for different nominal screw diameters,

every tick or cross representing one screw. Although these results present poor statistical significance, they confirm that the current formulation is unacceptable for smaller diameter screws and suggest, as expected, that larger screws do not require such high specific mechanical properties for successful use.

Most encountered criticalities involve the presence of bubbles or issues with the drive. Most broken screws fractured at the neck, and presented along the fracture surface one or more bubbles visible by eye. These bubbles could either have been already present in the composite as observed previously, or could have been introduced by the screwdriver when imprinting the drive's cross shape during curing. Cavities were also occasionally observed in two cases where the screw fractured in the shank while applying only a minimal torsion. In the case of larger samples such as the ones solicited to 3-point bending or the fixation patches used by *Hutchinson et al.*[3] the presence of porosity may affect the mechanical properties but is not so critical, as satisfactory results are still achievable. For the case of screws, however, the presence of residual porosity appears to be unacceptable and especially detrimental for lower diameter screws, as a single bubble can significantly reduce the resisting area along the shank or in the neck, leading to premature failure. Although lacking statistically sound data, the screws made of unfilled thermoset appear to be more resistant than those made with the prototype composite. This is attributable to two main factors: Firstly, the thermoset is significantly less viscous than the composite, lowering the risk of bubbles formation along the shank, secondly the strength of the thermoset is significantly higher than that of the prototype composite.

Off-centred drives also appeared to cause some problems: not being able to impress the drive perfectly along the screw's axis causes,during insertion, increased complex stresses that could further contribute to premature failure. Overall, higher mechanical properties are required for cortical screws.

Table 4.1.b: Thermoset or 56HA composite screws insertion in tapped porcine metacarpals outcomes

Diameter [mm]	2.0	2.5	3.5	4.0
56HA	❌❌❌❌	✅❌❌❌❌	❌✅	✅
Unfilled	❌❌❌❌	✅✅❌	✅✅	✅

4.2 Different fillers as reinforcing agents

As a first attempt to improve the mechanical properties of the composite, HA was replaced with different fillers, namely bioglass 58S (Bgl), hydroxyapatite whiskers (HA-w), and an apatitic powder known as “MCD apatitic abrasive” [84]. MCD was chosen due to it being a sintered apatitic material, therefore having superior mechanical properties to porous, supposedly unsintered, HA aggregates. HA-w, (elastic modulus 70-140 GPa [85,86]) were chosen using a similar rationale, but adding the fact that particles with a higher aspect ratio are known to be more effective reinforcing agents, thanks to the increased shear and bending stress transfer as well as higher specific surface area [56]. Bioglass, on the other hand, was chosen to introduce a resorbable component in the composite formulation, in view of a completely resorbable system. Bioactive glass is being extensively studied in fields such as dentistry and especially in regenerative medicine due to its osteoinductive properties [87].

Firstly, the maximum amount of filler that the TMTATOxTATATO thermoset could incorporate was evaluated. This was defined as the weight fraction of filler that could be added to the monomers to obtain the same pre-curing viscosity of TMTATOxTATATO 56HA and were determined to be 36, 58 and 62 wt.% respectively for Bgl, HA-w, and MCD. The viscosity determination was performed visually.

The mechanical properties of the composites with the different maximal filler loadings are presented in *Table 4.2* below. The most promising filler appeared to be HA-w, which increased the flexural modulus and strength respectively by 37% and 20% with respect to the standard composite. The formulation with sintered apatitic abrasive on the other hand exhibited the worst strength performance, as increasing particulate filler loading with no interfacial adhesion effectively decreased the resisting area[57,63]. The formulation with bioglass exhibited the lowest modulus, which was expected, as its modulus and volume loading were significantly lower compared to the apatitic fillers.

Table 4.2: Mechanical properties of TMTATOxTATATO with maximal different fillers

Filler and loading	E_f [GPa]	σ_f [MPa]	Flex strain [mm/mm $\cdot 10^{-3}$]	Energy at break [mJ]
56HA - standard	6.6 (0.1)	59 (1)	9.6 (0.2)	11.4 (0.2)
36 Bgl	4.5 (0.3)	50 (3)	11.5 (0.4)	11.5 (0.9)
58 HA-w	9.1 (0.2)	71 (3)	9.6 (0.5)	11.8 (1.1)
62 MCD	5.5 (0.3)	43 (2)	11.0 (0.1)	11.0 (0.1)

To further elucidate these results and correlations between mechanical properties and microstructure, the fracture surfaces were observed with a tabletop SEM. *Figure 4.2* presents some images of the fractured surfaces of the composite with MCD (a), Bgl (b), and HA-w (c,d). The spacing between MCD particles and the matrix clearly shows how poor the interaction between these two components is. The main reason that MCD yielded lower mechanics compared to the standard formulation is likely traceable to mechanical interlocking between matrix and particles, which could play a role when using HA fillers, but is excluded when using dense, smooth particles such as MCD. Due to MCD exhibiting the worst mechanical properties and not being resorbable, it was excluded from further investigations.

The HA-w polymer interface shown in *Figure 4.2 (d)* appeared as poor as the one for HA. Consequently, interfacial adhesion isn't likely to be a contributing factor to reinforcement. A reasonable explanation might lie in the geometrical mechanics of the TMTATOxTATATO 58HA-w system: as the HA-w have an elastic modulus about two orders of magnitude larger than the unfilled matrix, we can approximate them to undeformable rods immersed in a deformable matrix. When applying a load on the composite, the matrix will deform, albeit slightly, and due to the high aspect ratio of whiskers, form points of contact with the latter, through which more effective stress transfer can be achieved. Since the whiskers are not preferentially oriented, this phenomenon can occur regardless of the load application mode, granting isotropic reinforcement.

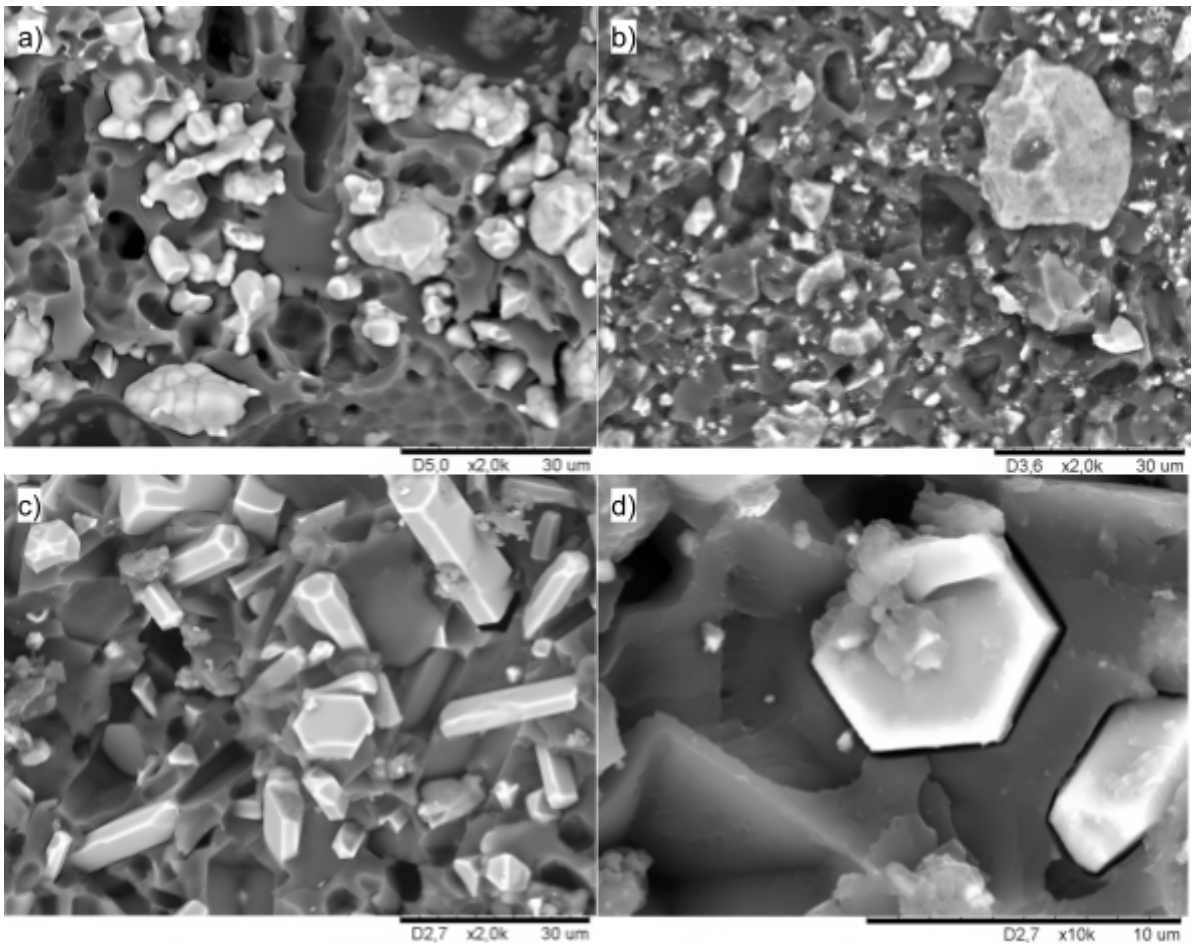

Figure 4.2: SEM images of TMTATOxTATATO filled with MCD (a), Bgl (b), HA-w (c,d)

4.3 Thiol-ene composite degassing

As a strategy to reduce porosity in the material before curing, a degassing step seemed to be the most easily applicable at a lab scale, with no special equipment required. After mixing of the components and filler, the composite was therefore placed in Schlenk line vacuum for 1.5 h .ca, after which it was cast and cured. The results of 3PB for degassed composites with 58HA-w and 56HA are presented in *Table 4.3*, comparing them against their non-degassed counterparts. In both cases, degassing resulted in superior mechanical properties and was therefore added to the standard composite production procedure.

Table 4.3: Mechanical properties of conventional vs degassed TMTATOxTATATO composites

Formulation	E_f [GPa]	σ_f [MPa]	Flex strain [mm/mm $\cdot 10^{-3}$]	Energy at break [mJ]
56HA	6.6 (0.1)	59 (1)	9.6 (0.2)	12 (2)
56HA degas	7.5 (0.5)	58 (5)	9.0 (0.4)	9 (1)
58 HA-w	9.1 (0.2)	71 (3)	9.6 (0.5)	12 (1)

58 HA-w degas	9.4 (0.3)	81 (5)	10.2 (0.5)	15 (2)

Interestingly however, the change in mechanical properties appears to be different between the formulations with HA and HA-w. While the samples with 56 HA showed an increase in flexural modulus (.ca 14%) but not in flexural strength, the opposite occurred for samples filled with 58HA-w, where the average flexural strength increased by .ca 14%, but no significant changes to the modulus were observed. A possible explanation for this phenomenon lies once again in the structural differences of the fillers. As HA is supposedly in an aggregate porous form, upon the application of a vacuum, the polymeric matrix will partly penetrate in the porous structure due to the pressure gradient generated as the air exits the pores. The lack of an increase in strength could be attributable to the limited cohesive strength of the aggregates, which might be the strength limiting factor or could play a role as stress-concentration points..

HA-w, on the other hand, cannot benefit from polymer matrix interlocking. The vacuum however, might reduce the gap between matrix and whiskers, improving load transfer, which combined with an overall porosity reduction could explain the increase in strength. However, the main beneficial mechanism is thought to be the reduction of porosity (and consequently the increase in resisting area), but further investigations would be required to confirm this.

The reduction in porosity can be clearly appreciated in *Figure 4.3*, where the fracture surfaces of untreated composites with 58HA-w (a,b) are compared with their degassed counterpart (c).

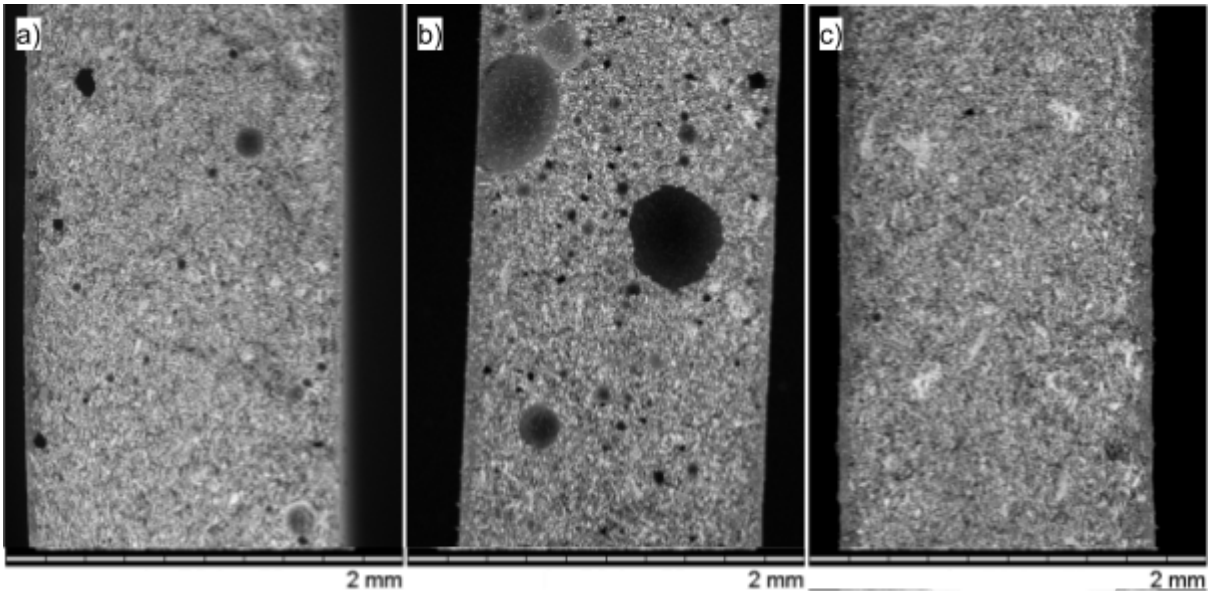

Figure 4.3: fracture surface of TMTATOxTATATO 58HA-w without (a: best sample, b worst sample) and with (c) degassing

4.4 Functionalized fillers as reinforcing agents

Following the rationale introduced previously, two different fillers were chosen to investigate the effect of their functionalization on the mechanical properties of the cured composite. HA-w and Bgls were chosen as promising candidates respectively due to their mechanical or resorbable properties. *Figure 4.4* displays the molecules chosen as promising compatibilization agents for the utilised fillers. Bgl was silanized with γ-MPS as it is routinely used for glass silanization in dental composites and exhibits amongst the highest strengthening properties [68]. Furthermore, the methacrylic tail provides a C-C double bond that can co-polymerize with TMTATO during curing, covalently bonding the Bgl particles with the polymer matrix.

HA-w on the other hand were functionalized with 2 different phosphonic acids, PEMPA and UEMPA. Phosphonic acids were chosen over organosilanes as, compared to them, they form a more stable bond with non-silica-based oxides [75,76]. Phosphonic acids with a terminal vinyl group were selected in order to allow for its copolymerization with TMTATO and ultimately the matrix, similarly to γ-MPS. They were also chosen with different lengths of the unsaturated tails as this was thought to be a parameter influencing their affinity towards the polymer phase and ultimately their compatibilizing effectiveness.

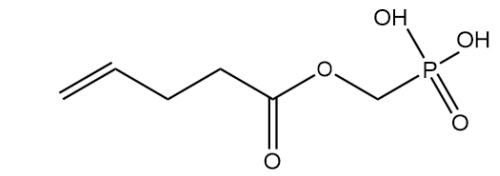

((pent-4-enoyloxy)methyl)phosphonic acid (PEMPA)

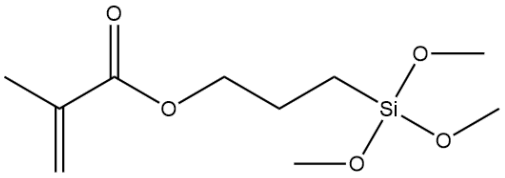

γ-methacryloxypropyltrimethoxysilane (γ-MPS)

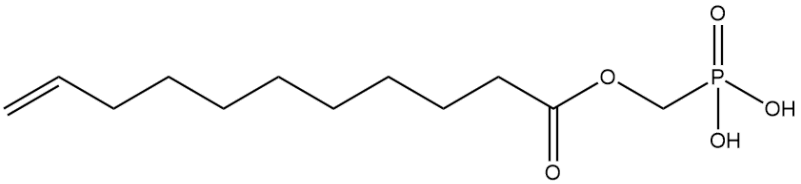

((undec-10-enoyloxy)methyl)phosphonic acid (UEMPA)

Figure 4.4: compatibilizing molecules used in this project

Composite beams were produced with 58wt% HA-w functionalized with PEMPA and UEMPA, as well as 36wt% Bgls functionalized with γ-MPS. All composites underwent the

degassing procedure. The results of three point bending tests are presented in *Table 4.4* comparing them to their unfunctionalized degassed counterparts.

The composites with functionalized HA-w didn´t show an improvement of their mechanical properties. Quite surprisingly, they actually appear to display a slightly lower flexural modulus, significant only for UEMPA, while all other properties remain unchanged. The causes of this adverse effect have not been investigated due to time constraints, however they might be similar to those experienced by *Altan et al.* [88], where some compatibilizers led to aggregation of particles and less efficient dispersion. Other possibilities might include a poor interaction between the compatibilizer and the TMTATO, hindering co-polymerization.

On the other hand, the composite with silanized bioglass exhibited remarkable enhancements of all mechanical properties, stiffness having the most modest of only about 20%. Flexural strength increased 120%, strain to break 160%, and energy at break .ca 500%. Energy at break is an especially important parameter, as it is closely linked to the impact resistance and brittleness of a material. While bone fixation screws are not expected to undergo significant impacts after implantation, having a high toughness greatly facilitates the surgeons' handling, lowering the risk of unwanted breakage. Confronting it with HA-w formulation, it presents only about 60% of its modulus, but strength and energy at break increase by nearly 40% and 400% respectively.

SEM observations of the fracture surfaces would have been desirable but were not possible due to instrument failure and time constraints.

Table 4.4: Mechanical properties of TMTATOxTATATO composites with functionalized vs unfunctionalized fillers, degassed.

Sample	E_f [GPa]	σ_f [MPa]	Flex strain [mm/mm $\cdot 10^{-3}$]	Energy at break [mJ]
36Bgl	4.5 (0.3)	50 (3)	11.5 (0.4)	11.5 (0.9)
36Bgl+γ-MPS	5.4 (0.1)	111 (8)	30 (0.4)	73(28)
58HA-w	9.4 (0.3)	81 (5)	10.2 (0.5)	15 (2)
58HA-w+PEMPA	8.5 (0.6)	81 (6)	10.3 (0.6)	15 (2)
58HA-w+UEMPA	8.1 (0.3)	79 (3)	10.7 (0.9)	16 (2)

4.5 Effect of filler loading on mechanical properties

For completeness' sake, the influence of filler loading on TMTATOxTATATO composites was evaluated for HA-w (10, 20, 30, 40, 50, 58 wt%) and Bgl+γ-MPS (25, 36 wt%), and is presented in *Figure 4.5.* The data points for Bgl+γ-MPS were limited due to supply limitations of the filler. As expected, by increasing the filler loading, the elastic modulus also increased for both filler types. The effects on flexural strength however, are radically different: while increasing the HA-w content decreased the flexural strength, seemingly reacting a plateau between 40 wt% and 58 wt%, increasing the content of silanized Bgl not only does not reduce the flexural strength, but increases its upper bound, albeit having a wide standard deviation. This enhancement, or non-loss, in strength is in line with the particulate reinforcement theories previously mentioned, highlighting the importance of a good interfacial bond in PRPMCs.

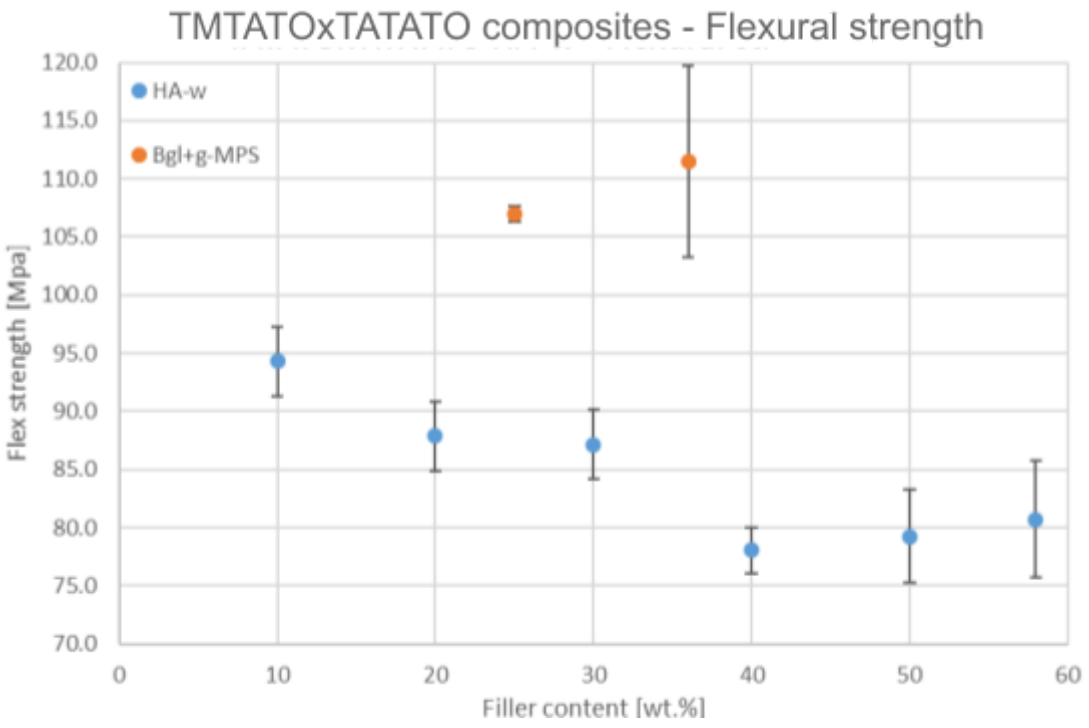

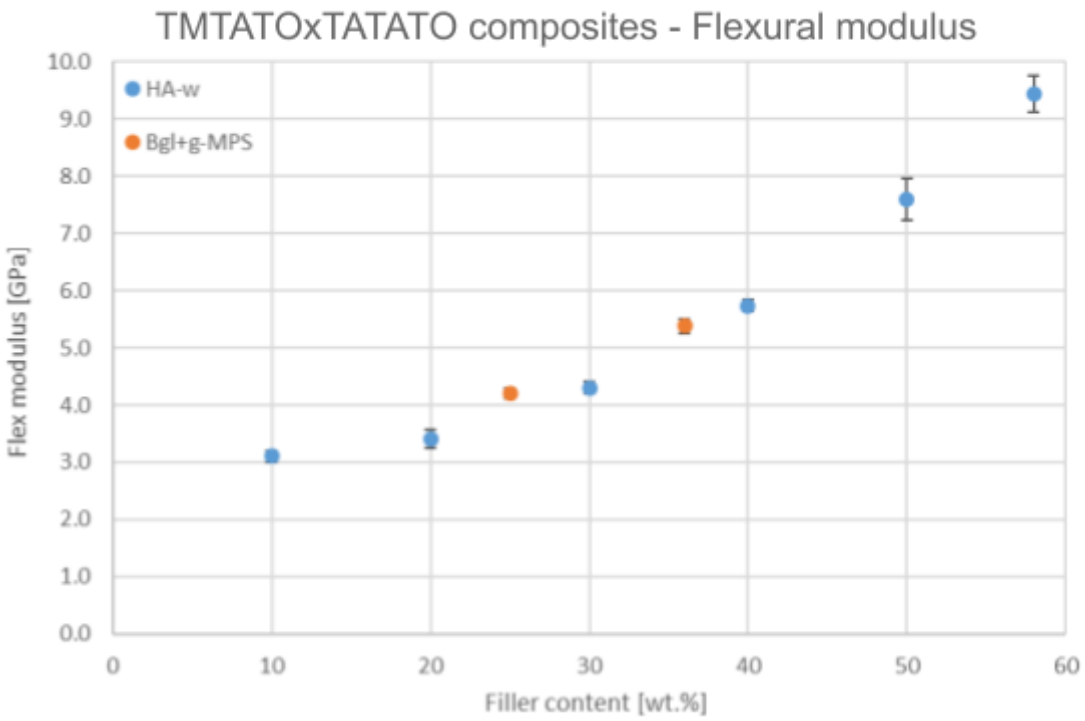

Figure 4.5: Mechanical properties of TMTATOxTATATO composites as a function of different fillers (BGL+γ-MPS: orange; HA-w: blue) loading

4.6 Preliminary cell viability

Preliminary cytotoxicity studies were performed on both the cured composites (with 58HA-w and 36Bgl+γ-MPS as fillers) and on the inorganic fillers themselves as described in section 3.2.8. The results of HaCaT cell viability are presented in *Figure 4.6,* with the composites shown. None of the samples of fillers nor composites showed any cytotoxic effects after 48 hours. Surprisingly, it appears that lower concentrations of pure fillers show lower cell viability, although only the difference for HA-w is statistically significant. Such a counterintuitive outcome cannot be explained logically by the author and is most likely attributable to the minimal practical experience in performing resazurin cell viability assays.

Although a more in-depth study should be performed to investigate the potential cytotoxicity of the newly formulated composites, these preliminary results suggest that they are not cytotoxic. This hypothesis is supported by the fact that both HA-w and silanized Bgls have been used as fillers in numerous studies and found to show good biocompatibility, both *in vitro* and *in vivo* [89–92], as well as the TMTATOxTATATO matrix [3]. Clearly, if these fillers will be used with a different polymer matrix, possibly resorbable, new cytotoxicity studies should be performed to test for potential matrix-filler interactions.

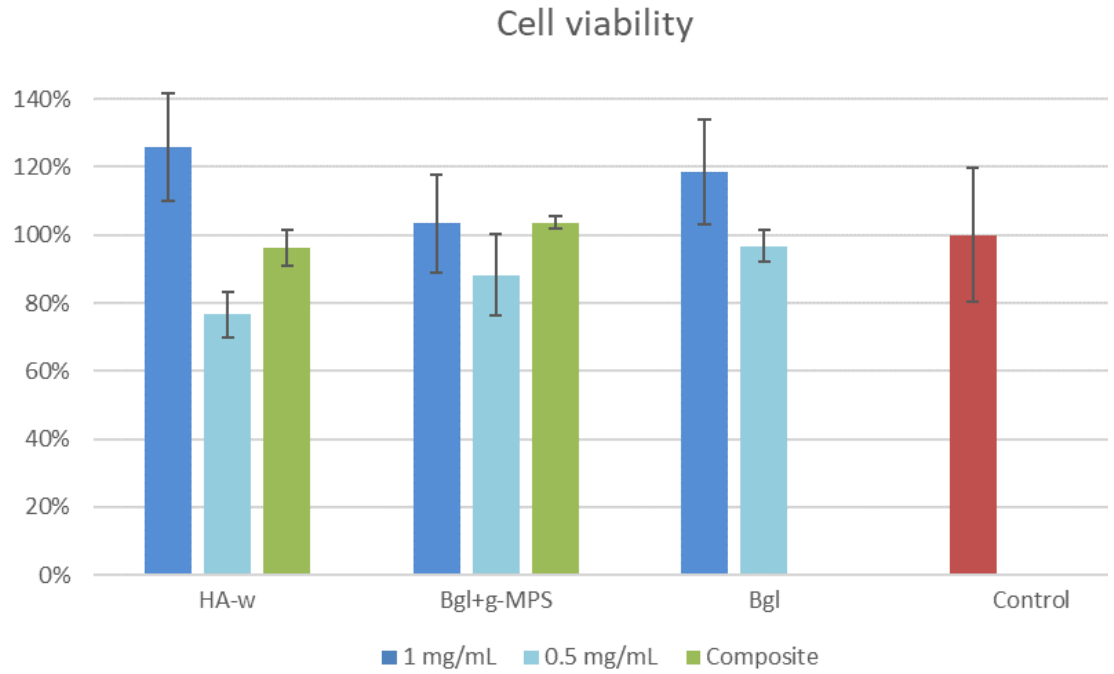

Figure 4.6: Cell viability of TMTATOxTATATO composites with 36 Bgls+γ-MPS, 58HA-w, as well as only the fillers at concentrations of 1 and 0.5 mg/mL

4.8 Materials platform comparison

The addition of a degassing step, as well as the introduction of silanized Bgl or HA-w, has pushed forward AdhFix formulations' mechanical properties boundaries, increasing toughness and strength or elastic modulus respectively. *Figure 4.7* presents a strength-modulus Ashby diagram of the AdhFix formulations containing 56HA with or without degassing, non-degassed 36BGL, degassed 36BGL+γ-MPS, degassed 58HA-w. Values for a previously developed unfilled thiol-yne polymer [44], commercially available polymers namely PLA and a PLA/PGA fibres 70:30 composite [93] , as well as PEEK [94], are also Included. The values of the strongest known resorbable composite (i.e. used in SuperFIXSORB-MX®) are not included as out of the chart, but were already reported in section 2.2.3 as flexural modulus and strength of 12 GPa and 270 MPa respectively[43].

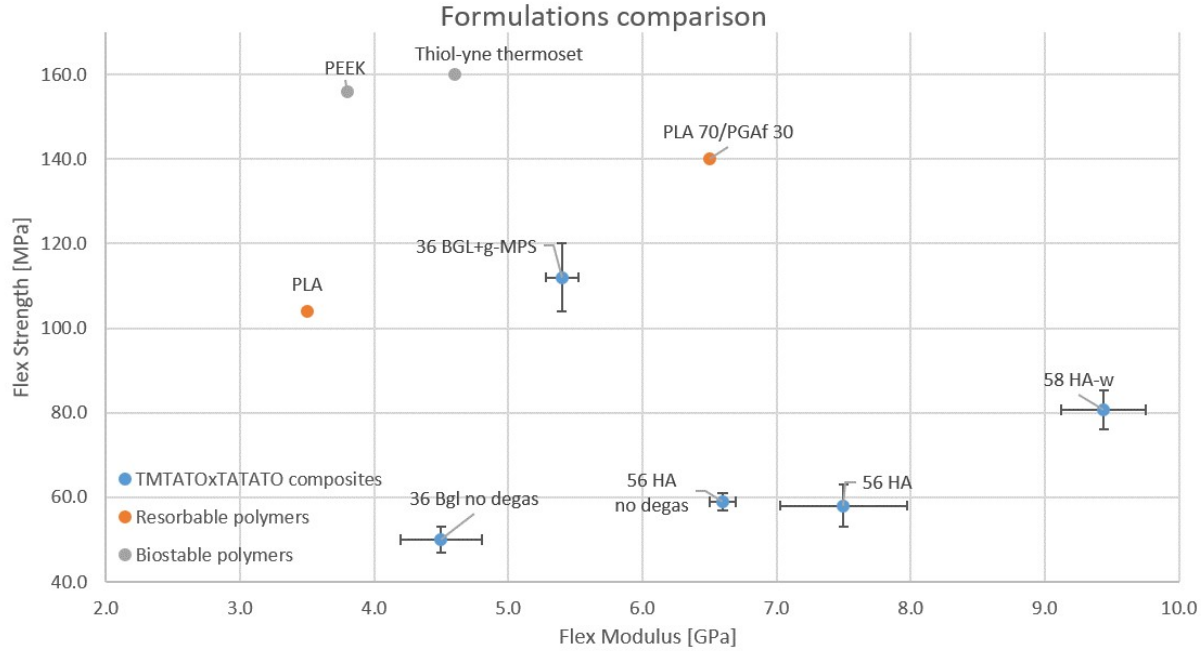

Figure 4.7: mechanical properties of various AdhFix formulations, thiol-yne thermoset, and commercially available biomedical polymeric materials.

4.8 Functional group concentration

Observing the FT-IR spectra of Bgl+γ-MPS vs clean Bgl in *Figure 4.8* two peaks can be observed in the magnified section. The wide signal around 1480-1520 cm^{-1} is attributable to v_3 vibrational mode of the carbonate structures which are formed as the bioglass is exposed to water and CO_2[95–98]. The smaller signal around 1690-1730 cm^{-1} is instead attributable to the stretching of the carbonyl in γ-MPS, suggesting a successful silanization of the Bgl particles[99]. It is not possible however, through these readings only to quantify the silane molecules concentration.

On the other hand, determining the outcome of the compatibilization reactions of HA-w has proven to be a non-trivial task. The allyl groups in UEMPA and PEMPA could not be observed either via FT-IR nor via Raman spectroscopy. The method described in Section determination of functional groups concentration was therefore developed to obtain quantitative estimates of surface allyl group concentration. Photocatalysed thiol-ene coupling was chosen because, as explained previously, it generates near-100% yields, with limited side reactions and in a short time. 3,6-Dioxa-1,8-octane-dithiol was selected as the most readily available dithiol in the lab, but any dithiol is potentially a good candidate for this method. DTNB was chosen as a well-proven and readily available colorimetric method for detection of thiol groups[100].

The calculations were made by assuming that all allyl groups coupled one-to-one with di-thiol molecules. *Table 4.8* presents the functional group concentration relative to HA-w functionalized with PEMPA and UEMPA, as well as the values for Bgl functionalized with γ-MPS. These values are expressed in micromoles of allyl moieties per gram of filler.

As expected, the functionalization concentration of the phosphonic acids on HA-w is comparable. The functional group concentration on BGL on the other hand, is .ca 25 times larger than on HA-w. Such a large difference could stem from three different factors, the first being the difference in specific surface area between BGL particles and HA-w. Secondly, a higher surface allyl concentration could be due to the formation of a 3D multilayer of the silane as explained in section 2.4.1 which could accommodate more compatibilizers than a bidimensional monolayer. Lastly, the phosphonic acids could have reacted only partly with the whiskers, not forming a dense monolayer. Further investigations in this sector should be performed for future developments.

Table 4.8: Allyl group concentration

Sample	Functionalization (µmol/g)
HA-w+PEMPA	0.25
HA-w+UEMPA	0.27
BGL+γ-MPS	6.7

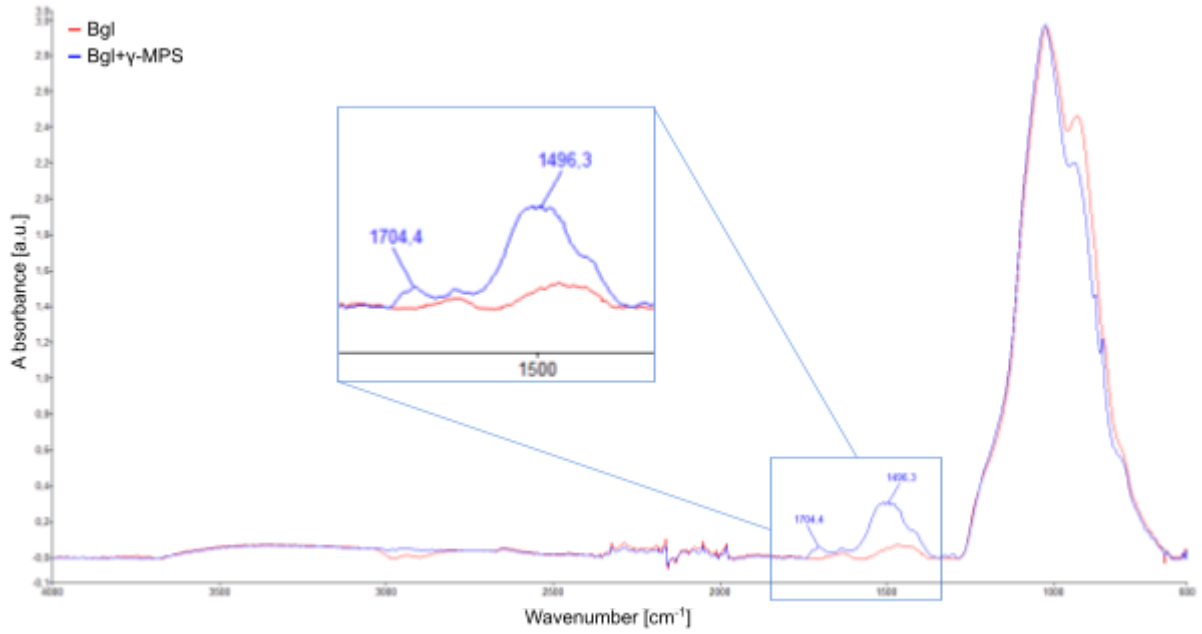

Figure 4.8: FT-IR spectra of BGL before (red) and after (blue) functionalization with γ-MPS

4.9 Porcine fracture model

Bicortical composite screws were produced with diameters of 1.5 and 2.5 mm using TMTATOxTATATO 36Bgls+γ-MPS. This formulation was chosen as it displayed the highest flexural strength and work at break, therefore reducing the risk of accidental break due to

mishandling during their insertion. They were then used in place of metal screws for the AdhFix procedure on porcine metacarpals. The qualitative difference with respect to the screws fabricated in section 4.1 was clear, as out of the fourteen 1.5 mm screws containing Bgl+γ-MPS, only two broke during insertion, compared to all TMTATOxTATATO 56HA 2mm screws as per *Table 4.1.b*. Of these two, one had a large bubble in the shank at the fracture surface, while the other broke due to mishandling by applying a shear stress via involuntary hand movement. Although these results exhibit great improvement with respect to the conventional formulation, the sensitivity of such screws to unintentional loads represents a major drawback for clinical application. Increasing the size of the screws of only 1 mm however, grants them far superior resistance and mechanical properties, suggesting that their use could be considered for larger fractures.

Figure 4.9 (L) presents the 3PB results of porcine metacarpal model fractures fixated with TMTATOxTATATO 36Bgl+γ-MPS, and secured to bones with either metal screws (Ti6Al4V) of 1.5 mm diameter or composite screws of 1.5 or 2.5 mm diameter. On the right (R), the results are normalised with respect to the fractures' surface area to obtain values that take into account, although roughly, the thickness of the patch.

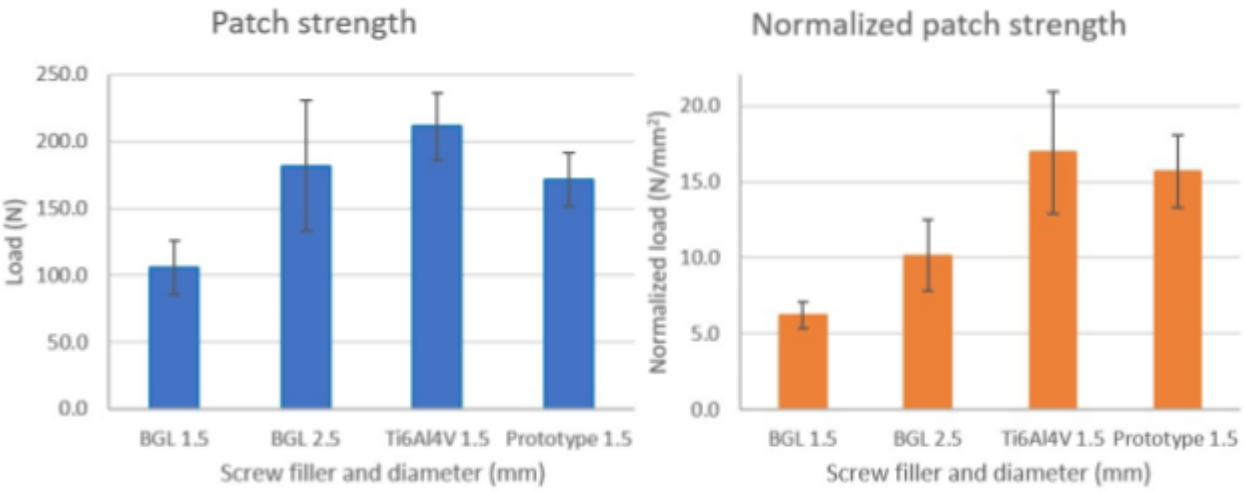

Figure 4.9: TMTATOxTATATO *36BGL*+γ-MPS *BFPs strength (L) and normalized strength (R) with different screws (from left to right: 1.5 and 2.5 mm composite, 1.5 mm metal) compared against the BFPs of prototype composite with 1.5 mm metal screws.*

These results clearly show that the strength of fully composite BFPs are limited by the screws' size. BFPs with 2.5 mm screws showed in fact a significant increase in strength, achieving comparable results with those using metal screws. The normalized strength appears to confirm this trend, although a larger difference is apparent between the BFPs with metal screws and the 2.5 mm composite ones. 1.5 mm screws being the strength limiting factor is further supported by their necks' breakage during testing, leading to BFP

detachment. As opposed to the 2.5 mm composite ones, which showed breakage of the patch itself. In the latter case the fracture comprised the patch-screwhead interphase, as in the case of metal screws, suggesting that such region either offers lower strength than the bulk patch or acts as a stress-concentration region.

Although the fully composite systems appear less strong than the prototype BFPs, the BFPs made from the newly developed formulation with BGL+γ-MPS show comparable, maximally higher, strength despite the introduction of resorbable components. Furthermore, although they possess the lowest strength, the fully composite BFPs with 1.5 mm screws are still equivalent, if not superior, to the strength of k-wires, which yield at 80 (6) N [3].

4.10 Considerations and future work suggestions

As reported previously [3], the chemical composition of TMTATOxTATATO makes it a non-degradable polymer once cured. A first step to introduce biodegradability in this fixation system was taken by replacing HA with silanized Bgl. The resorption speed of bioglass depends intrinsically on its composition, and can be tailored by varying the amount of glass-network modifiers (e.g. Na_2O) in the material or by modifying the particles' geometry [101]. When used immersed in a polymer matrix, the overall degradation rate of the composite will be determined by factors other than the single degradation rate of the two isolated components. The presence of a Bgls could in fact hinder or promote the water permeation and absorption of the composite, or attract cells involved in bone formation and remodelling (e.g. osteoblasts, osteoclasts) that could further alter the degradation by secreting extracellular substances or by micromechanical stimuli. For this reason, any developed composite should thoroughly undergo degradation studies. Overall, the introduction of bioglass shows promising mechanical properties as a resorbable reinforcing agent for TE resorbable composites.

The introduction of HA-w, on the other hand, is not considered to enhance resorbability of the composite, as HA-w are mostly inert [27], but has shown the potential to improve the mechanical properties in non-resorbable formulations, which are currently the AdhFix standard. The two compatibilizing molecules here synthesised have not proven to be effective in enhancing mechanical properties of the composite and different structures should be considered, perhaps including a methacrylate group as in the tail of γ-MPS or changing the class of molecules altogether.

This project has been conducted screening a wide range of variables, and time constraints made it so that a limited number of repetitions could be conducted for each measurement

(e.g. only 3 BFPs for each screw-formulation pair). No statistical analysis has therefore been performed on the data and only the standard deviation was reported. Any future work should therefore include more data readings to be able to include quantitative statistical conclusions rather than qualitative only.

5. Conclusions

As the currently employed AdhFix prototype formulation does not possess satisfactory mechanical properties for small size screw production, three different routes were investigated to tackle this: changing the filler, adding a degassing step and functionalizing the fillers with allyl-containing compatibilizers.

Substitution of HA porous particles with hydroxyapatite whiskers (HA-w) showed the greatest improvements among the fillers screened, improving flexural strength and modulus by 20% and 37% respectively. All the fillers showed poor adhesion with the TMTATOxTATATO matrix, but the porous structure of HA can give rise to mechanical interlocking, while the high aspect ratio of HA-w granted more contact points. The formulation with unfunctionalized BGL had the lowest modulus due to its lower filler loading.

The addition of a degassing step was found to significantly reduce the material's porosity, although the effects on the final mechanical properties appear to be dependent on the filler's morphology. For dense fillers, the suggested effect is an increase of the resisting area, in turn improving strength. For porous fillers, a vacuum could additionally promote mechanical interlocking, favouring stress transfer.

Functionalization of the fillers yielded mixed results. BGL functionalized with γ-MPS and degassed greatly improved the mechanical properties, such as 120% increase in flexural strength and 500% increase in energy at break. On the other hand, HA-w functionalized with phosphonic acids didn't show any improvement in reinforcing abilities. The causes of failed compatibilization were not addressed in this project, although it is suggested that might be related to low specific surface area, incomplete functionalization, or inadequate interaction between the compatibilizer and the polymer matrix.

Lastly, screws of ∅ 1.5 and 2.5 mm were casted out of TMTATxTATATO 36BGL+γ-MPS to test fully composite bone fixation patches. Their strength was found to be limited by the screws when using 1.5 mm ones although they still exceeded the yielding strength of K-wires. Fully composite BFPs with 2.5 mm screws displayed strength comparable, if not superior, to BFPs made with the prototype formulation with metal screws. Overall it has been

demonstrated that a customisable, fully-composite, bone fixation system can be obtained based on thiol-ene matrix. Furthermore, the introduction of resorbable phases did not compromise the strength of the BFPs.

6. Bibliography

[1] Wu, A.-M. et al. (2021). Global, regional, and national burden of bone fractures in 204 countries and territories, 1990–2019: a systematic analysis from the Global Burden of Disease Study 2019. *The Lancet Healthy Longevity*. DOI: 10.1016/S2666-7568(21)00172-0.

[2] Guerrero, E.M. et al. (2021). Complications of Low-Profile Plate Fixation of Phalanx Fractures. *Hand (New York, N.Y.)*. DOI: 10.1177/1558944719855684.

[3] Hutchinson, D.J. et al. (2021). Highly Customizable Bone Fracture Fixation through the Marriage of Composites and Screws. *Advanced Functional Materials*. DOI: 10.1002/adfm.202105187.

[4] Hernigou, P. and Pariat, J. (2017). History of internal fixation (part 1): early developments with wires and plates before World War II. *International Orthopaedics*. DOI: 10.1007/s00264-016-3347-4.

[5] Anderson, J.M. et al. (2008). Foreign body reaction to biomaterials. *Seminars in Immunology*. DOI: 10.1016/j.smim.2007.11.004.

[6] Wei, Q. et al. (2014). Protein Interactions with Polymer Coatings and Biomaterials. *Angewandte Chemie International Edition*. DOI: 10.1002/anie.201400546.

[7] Davis, R. et al. (2022). A comprehensive review on metallic implant biomaterials and their subtractive manufacturing. *The International Journal of Advanced Manufacturing Technology*. DOI: 10.1007/s00170-022-08770-8.

[8] Sansone, V. et al. (2013). The effects on bone cells of metal ions released from orthopaedic implants. A review. *Clinical Cases in Mineral and Bone Metabolism*. DOI: 10.11138/ccmbm/2013.10.1.034.

[9] Ibrahim, H. et al. (2017). Resorbable bone fixation alloys, forming, and post-fabrication treatments. *Materials Science and Engineering: C*. DOI: 10.1016/j.msec.2016.09.069.

[10] Morgan, E.F. et al. (2018). Bone Mechanical Properties in Healthy and Diseased States. *Annual review of biomedical engineering*. DOI: 10.1146/annurev-bioeng-062117-121139.

[11] Karl, J.W. et al. (2015). The Epidemiology of Upper Extremity Fractures in the United States, 2009. *Journal of Orthopaedic Trauma*. DOI: 10.1097/BOT.0000000000000312.

[12] VAN ONSELEN, E.B.H. et al. (2003). Prevalence and Distribution of Hand Fractures. *Journal of Hand Surgery*. DOI: 10.1016/S0266-7681(03)00103-7.

[13] Page, S.M. and Stern, P.J. (1998). Complications and range of motion following plate fixation of metacarpal and phalangeal fractures. *The Journal of Hand Surgery*. DOI: 10.1016/S0363-5023(98)80157-3.

[14] Kurzen, P. et al. (2006). Complications after Plate Fixation of Phalangeal Fractures. *Journal of Trauma and Acute Care Surgery*. DOI: 10.1097/01.ta.0000214887.31745.c4.

[15] von Kieseritzky, J. et al. (2017). Reoperations and postoperative complications after osteosynthesis of phalangeal fractures: a retrospective cohort study. *Journal of Plastic Surgery and Hand Surgery*. DOI: 10.1080/2000656X.2017.1313261.

[16] Adams, J.E. et al. (2013). The Biomechanics of Fixation Techniques for Hand Fractures. *Hand Clinics*. DOI: 10.1016/j.hcl.2013.08.004.

[17] (2018). K Wire Fixation of Hand Fractures.

[18] Stern, P.J. et al. (1987). Complications of Plate Fixation in the Hand Skeleton. *Clinical Orthopaedics and Related Research (1976-2007)*.

[19] Shanmugam, R. et al. (2015). Angular stable lateral plating is a valid alternative to conventional plate fixation in the proximal phalanx. A biomechanical study. *Clinical Biomechanics*. DOI: 10.1016/j.clinbiomech.2015.03.019.

[20] Fischer, K.J. et al. (1999). Low-profile versus conventional metacarpal plating systems: A comparison of construct stiffness and strength. *The Journal of Hand Surgery*. DOI: 10.1053/jhsu.1999.0928.

[21] https://journals.lww.com/jbjsjournal/Citation/1979/61050/Tendon_rupture_as_a_complication_of_screw_fixation.26.aspx.
[22] Farah, S. et al. (2016). Physical and mechanical properties of PLA, and their functions in widespread applications — A comprehensive review. *Advanced Drug Delivery Reviews*. DOI: 10.1016/j.addr.2016.06.012.
[23] Van de Velde, K. and Kiekens, P. (2002). Biopolymers: overview of several properties and consequences on their applications. *Polymer Testing*. DOI: 10.1016/S0142-9418(01)00107-6.
[24] Budak, K. et al. (2020). A review on synthesis and biomedical applications of polyglycolic acid. *Journal of Polymer Research*. DOI: 10.1007/s10965-020-02187-1.
[25] Liao, C. et al. (2020). Polyetheretherketone and Its Composites for Bone Replacement and Regeneration. *Polymers*. DOI: 10.3390/polym12122858.
[26] Oonishi, H. et al. (1997). Particulate Bioglass Compared With Hydroxyapatite as a Bone Graft Substitute. *Clinical Orthopaedics and Related Research®*.
[27] Trzaskowska, M. et al. (2023). The Impact of Hydroxyapatite Sintering Temperature on Its Microstructural, Mechanical, and Biological Properties. *International Journal of Molecular Sciences*. DOI: 10.3390/ijms24065083.
[28] Chen, Q.Z. et al. (2006). 45S5 Bioglass-derived glass-ceramic scaffolds for bone tissue engineering. *Biomaterials*. DOI: 10.1016/j.biomaterials.2005.11.025.
[29] Kucko, S.K. et al. (2022). Current Advances in Hydroxyapatite- and β-Tricalcium Phosphate-Based Composites for Biomedical Applications: A Review. *Biomedical Materials & Devices*. DOI: 10.1007/s44174-022-00037-w.
[30] Jones, J.R. (2013). Review of bioactive glass: From Hench to hybrids. *Acta Biomaterialia*. DOI: 10.1016/j.actbio.2012.08.023.
[31] Shikinami, Y. et al. (2005). The complete process of bioresorption and bone replacement using devices made of forged composites of raw hydroxyapatite particles/poly l-lactide (F-u-HA/PLLA). *Biomaterials*. DOI: 10.1016/j.biomaterials.2005.02.016.
[32] https://teijin-medical.co.jp.
[33] Landes, C.A. et al. (2006). Maxillary and Mandibular Osteosyntheses with PLGA and P(L/DL)LA Implants: A 5-Year Inpatient Biocompatibility and Degradation Experience. *Plastic and Reconstructive Surgery*. DOI: 10.1097/01.prs.0000218787.49887.73.
[34] https://www.jnjmedtech.com/en-EMEA/product/rapidsorb-resorbable-fixation-system.
[35] DePuy Synthes (2022). Resorbable Implants for Craniofacial Surgery.
[36] Inion Oy (2022). Inion CPS Bioabsorbable Fixation System Product Overview.
[37] Inion - Products - FreedomPlate™ Fracture Fixation System. *Inion*.
[38] Inion - Products - FreedomScrew™ Bioabsorbable Screw. *Inion*.
[39] Pietrzak, W.S. and Eppley, B.L. (2006). Stability of Craniofacial PLLA/PGA Copolymer Bioabsorbable Screws. *Journal of Craniofacial Surgery*.
[40] Johnston, M. et al. (2011). Resorption and Remodeling of Hydroxyapatite–Poly-L-Lactic Acid Composite Anterior Cruciate Ligament Interference Screws. *Arthroscopy: The Journal of Arthroscopic & Related Surgery*. DOI: 10.1016/j.arthro.2011.06.036.
[41] https://www.conmed.com/en-gb/products/implants-and-suture-anchors/interference-screws/bioscrew-bioabsorbable-interference-screws.
[42] https://www.conmed.com/en-gb/products/implants-and-suture-anchors/interference-screws/genesys-matryx-interference-screw.
[43] Shikinami, Y. and Okuno, M. (1999). Bioresorbable devices made of forged composites of hydroxyapatite (HA) particles and poly-L-lactide (PLLA): Part I. Basic characteristics. *Biomaterials*. DOI: 10.1016/S0142-9612(98)00241-5.
[44] Granskog, V. et al. (2018). High-Performance Thiol–Ene Composites Unveil a New Era of Adhesives Suited for Bone Repair. *Advanced Functional Materials*. DOI:

10.1002/adfm.201800372.
[45] Posner, T. (1905). Beiträge zur Kenntniss der ungesättigten Verbindungen. II. Ueber die Addition von Mercaptanen an ungesättigte Kohlenwasserstoffe. *Berichte der deutschen chemischen Gesellschaft*. DOI: 10.1002/cber.190503801106.
[46] Miwafern (2015). Thiol-ene radial addition step- and chain-growth mechanism.
[47] Hoyle, C.E. and Bowman, C.N. (2010). Thiol–Ene Click Chemistry. *Angewandte Chemie International Edition*. DOI: 10.1002/anie.200903924.
[48] Lee, T.Y. et al. (2007). Thiol−Allyl Ether−Methacrylate Ternary Systems. Polymerization Mechanism. *Macromolecules*. DOI: 10.1021/ma062494b.
[49] Hoyle, C.E. et al. (2004). Thiol–enes: Chemistry of the past with promise for the future. *Journal of Polymer Science Part A: Polymer Chemistry*. DOI: 10.1002/pola.20366.
[50] LaBauve, J.R. et al. (2012). What every dentist should know about bisphenol A. *General Dentistry*.
[51] Aminoroaya, A. et al. (2021). A review of dental composites: Challenges, chemistry aspects, filler influences, and future insights. *Composites Part B: Engineering*. DOI: 10.1016/j.compositesb.2021.108852.
[52] Arseneault, M. et al. (2018). The Dawn of Thiol-Yne Triazine Triones Thermosets as a New Material Platform Suited for Hard Tissue Repair. *Advanced Materials*. DOI: 10.1002/adma.201804966.
[53] Reinelt, S. et al. (2014). Synthesis and Photopolymerization of Thiol-Modified Triazine-Based Monomers and Oligomers for the Use in Thiol-Ene-Based Dental Composites. *Macromolecular Chemistry and Physics*. DOI: 10.1002/macp.201400174.
[54] Godara, S.S. et al. (2021). Review on history and characterization of polymer composite materials. *Materials Today: Proceedings*. DOI: 10.1016/j.matpr.2020.12.680.
[55] Egbo, M.K. (2021). A fundamental review on composite materials and some of their applications in biomedical engineering. *Journal of King Saud University - Engineering Sciences*. DOI: 10.1016/j.jksues.2020.07.007.
[56] Badini, C. (2013). *Materiali compositi per l'ingegneria*, CELID.
[57] Ahmed, S. and Jones, F.R. (1990). A review of particulate reinforcement theories for polymer composites. *Journal of Material Science*.
[58] Mooney, M. (1951). The viscosity of a concentrated suspension of spherical particles. *Journal of Colloid Science*. DOI: 10.1016/0095-8522(51)90036-0.
[59] Kerner, E.H. (1956). The Elastic and Thermo-elastic Properties of Composite Media. *Proceedings of the Physical Society. Section B*. DOI: 10.1088/0370-1301/69/8/305.
[60] Takayanagi, M. et al. (1964). Application of equivalent model method to dynamic rheo-optical properties of crystalline polymer. *Journal of Polymer Science Part C: Polymer Symposia*. DOI: 10.1002/polc.5070050111.
[61] Chow, T.S. (1978). EFFECT OF PARTICLE SHAPE AT FINITE CONCENTRATION ON THE ELASTIC MODULI OF FILLED POLYMERS. *J Polym Sci Polym Phys Ed*. DOI: 10.1002/pol.1978.180160602.
[62] Cox, H.L. (1952). The elasticity and strength of paper and other fibrous materials. *British Journal of Applied Physics*. DOI: 10.1088/0508-3443/3/3/302.
[63] Fu, S.-Y. et al. (2008). Effects of particle size, particle/matrix interface adhesion and particle loading on mechanical properties of particulate–polymer composites. *Composites Part B: Engineering*. DOI: 10.1016/j.compositesb.2008.01.002.
[64] Bouza, R. et al. (2011). Effect of particle size and a processing aid on the crystallization and melting behavior of iPP/red pine wood flour composites. *Composites Part A: Applied Science and Manufacturing*. DOI: 10.1016/j.compositesa.2011.03.022.
[65] Liang, J.Z. et al. (1999). Crystallization Behavior of Glass Bead-Filled Low-Density Polyethylene Composites. *Journal of Applied Polymer Science*. DOI: 10.1002/(SICI)1097-4628(19990131)71:5<687::AID-APP2>3.0.CO;2-Q.
[66] Packham, D.E. (2017). Theories of Fundamental Adhesion, in *Handbook of Adhesion*

Technology (eds.da Silva, L.F.M. et al.), Springer International Publishing, Cham, pp. 1–31.
[67] Comyn, J. (1997). *Adhesion Science*, Royal Society of Chemistry.
[68] Karkanis, S. et al. (2022). Effect of Silica Nanoparticles Silanized by Functional/Functional or Functional/Non-Functional Silanes on the Physicochemical and Mechanical Properties of Dental Nanocomposite Resins. *Applied Sciences*. DOI: 10.3390/app12010159.
[69] Wilson, K.S. et al. (2005). Systematic variation of interfacial phase reactivity in dental nanocomposites. *Biomaterials*. DOI: 10.1016/j.biomaterials.2005.01.008.
[70] Koleganova, V.A. et al. (2006). Bioactive glass/polymer composite materials with mechanical properties matching those of cortical bone. *Journal of Biomedical Materials Research Part A*. DOI: 10.1002/jbm.a.30561.
[71] Lung, C.Y.K. et al. (2016). Effect of silanization of hydroxyapatite fillers on physical and mechanical properties of a bis-GMA based resin composite. *Journal of the Mechanical Behavior of Biomedical Materials*. DOI: 10.1016/j.jmbbm.2015.09.033.
[72] Shuai, C. et al. (2020). Phosphonic Acid Coupling Agent Modification of HAP Nanoparticles: Interfacial Effects in PLLA/HAP Bone Scaffold. *Polymers*. DOI: 10.3390/polym12010199.
[73] Guo, Z. et al. (2006). Surface functionalized alumina nanoparticle filled polymeric nanocomposites with enhanced mechanical properties. *Journal of Materials Chemistry*. DOI: 10.1039/B603020C.
[74] Guerrero, G. et al. (2001). Anchoring of Phosphonate and Phosphinate Coupling Molecules on Titania Particles. *Chemistry of Materials*. DOI: 10.1021/cm001253u.
[75] Guerrero, G. et al. (2013). Phosphonate coupling molecules for the control of surface/interface properties and the synthesis of nanomaterials. *Dalton Transactions*. DOI: 10.1039/C3DT51193F.
[76] Kyriakou, N. et al. (2020). Hydrolytic stability of PEG-grafted γ-alumina membranes: Alkoxysilane vs phosphonic acid linking groups. *Microporous and Mesoporous Materials*. DOI: 10.1016/j.micromeso.2020.110516.
[77] Hubert Mutin, P. et al. (2005). Hybrid materials from organophosphorus coupling molecules. *Journal of Materials Chemistry*. DOI: 10.1039/B505422B.
[78] Antoniac, I. et al. (2013). Development of Bioabsorbable Interference Screws: How Biomaterials Composition and Clinical and Retrieval Studies Influence the Innovative Screw Design and Manufacturing Processes, in *Biologically Responsive Biomaterials for Tissue Engineering* (eds.Antoniac, I.), Springer, New York, NY, pp. 107–136.
[79] Schindelin, J. et al. (2012). Fiji: an open-source platform for biological-image analysis. *Nature Methods*. DOI: 10.1038/nmeth.2019.
[80] Massengill, J.B. et al. (1979). Mechanical analysis of Kirschner wire fixation in a phalangeal model. *The Journal of Hand Surgery*. DOI: 10.1016/S0363-5023(79)80073-8.
[81] Black, D.M. et al. (1986). The stability of internal fixation in the proximal phalanx. *The Journal of Hand Surgery*. DOI: 10.1016/S0363-5023(86)80010-7.
[82] https://www.bmglabtech.com/en/application-notes/ellmans-assay-for-in-solution-quantification-of-sulfhydryl-groups/.
[83] Aarthy, S. et al. (2019). Exploring the effect of sintering temperature on naturally derived hydroxyapatite for bio-medical applications. *Journal of Materials Science: Materials in Medicine*. DOI: 10.1007/s10856-019-6219-9.
[84] https://www.himed.com/mcd-apatitic-abrasive.
[85] Zamiri, A. and De, S. (2011). Mechanical properties of hydroxyapatite single crystals from nanoindentation data. *Journal of the mechanical behavior of biomedical materials*. DOI: 10.1016/j.jmbbm.2010.11.001.
[86] Teraoka, K. et al. (1998). Mechanical Properties of Hydroxyapatite and OH-carbonated Hydroxyapatite Single Crystals. *Journal of Dental Research*. DOI: 10.1177/00220345980770071201.

[87] Cannio, M. et al. (2021). Bioactive Glass Applications: A Literature Review of Human Clinical Trials. *Materials*. DOI: 10.3390/ma14185440.
[88] Altan, M. and Yildirim, H. (2012). Effects of compatibilizers on mechanical and antibacterial properties of injection molded nano-ZnO filled polypropylene. *Journal of Composite Materials*. DOI: 10.1177/0021998312436999.
[89] Zhang, H. et al. (2010). Biocompatibility and bioactivity of hydroxyapatite whiskers reinforced bis-GMA based composites. *2010 3rd International Conference on Biomedical Engineering and Informatics*. DOI: 10.1109/BMEI.2010.5639603.
[90] Xie, L. et al. (2016). Preparation, in vitro degradability, cytotoxicity, and in vivo biocompatibility of porous hydroxyapatite whisker-reinforced poly(L-lactide) biocomposite scaffolds. *Journal of Biomaterials Science, Polymer Edition*. DOI: 10.1080/09205063.2016.1140613.
[91] Salehi, S. et al. (2015). Cytotoxicity of Resin Composites Containing Bioactive Glass Fillers. *Dental materials : official publication of the Academy of Dental Materials*. DOI: 10.1016/j.dental.2014.12.004.
[92] Daguano, J.K.M.F. et al. (2013). Bioactivity and cytotoxicity of glass and glass–ceramics based on the 3CaO·P2O5–SiO2–MgO system. *Journal of Materials Science: Materials in Medicine*. DOI: 10.1007/s10856-013-4972-8.
[93] Ko, H.-S. et al. (2021). Mechanical Properties and Bioactivity of Poly(Lactic Acid) Composites Containing Poly(Glycolic Acid) Fiber and Hydroxyapatite Particles. *Nanomaterials*. DOI: 10.3390/nano11010249.
[94] Williams, D.F. et al. (1987). Potential of polyetheretherketone (PEEK) and carbon-fibre-reinforced PEEK in medical applications. *Journal of Materials Science Letters*. DOI: 10.1007/BF01728981.
[95] Perardi, A. et al. (2005). Carbonate formation on sol-gel bioactive glass 58S and on Bioglass® 45S5, in *Studies in Surface Science and Catalysis*, vol. 155, Elsevier, pp. 461–469.
[96] Xu, B. et al. (2018). Vibrational properties of isotopically enriched materials: the case of calcite. *RSC Advances*. DOI: 10.1039/C8RA06608F.
[97] Weng, J. et al. (1997). Formation and characteristics of the apatite layer on plasma-sprayed hydroxyapatite coatings in simulated body fluid. *Biomaterials*. DOI: 10.1016/S0142-9612(97)00022-7.
[98] Cerruti, M. and Morterra, C. (2004). Carbonate Formation on Bioactive Glasses. *Langmuir*. DOI: 10.1021/la049723c.
[99] Shirosaki, Y. et al. (2005). In vitro apatite formation on organic polymers modified with a silane coupling reagent. *Journal of The Royal Society Interface*. DOI: 10.1098/rsif.2005.0048.
[100] Winther, J.R. and Thorpe, C. (2014). Quantification of Thiols and Disulfides. *Biochimica et biophysica acta*. DOI: 10.1016/j.bbagen.2013.03.031.
[101] Ramaswamy, R. et al. (2022). Dissolution-precipitation reactions of silicate mineral fibers at alkaline pH. *Cement and Concrete Research*. DOI: 10.1016/j.cemconres.2022.106922.

Acknowledgements

First of all, I’d like to express my gratitude to my supervisors, Jorge and Dan, who helped and guided me through this project. A big thank you to my friends, for sharing this intense Swedish winter, and my family, for whom I was always too far. Appreciation is due to Eva for letting me find out about this project, and Michael for giving me this opportunity. Special appreciations also go to the whole division of coating technology at KTH, who welcomed me and always made me feel at home.